Unconventional Onshore Program RFP2007UN001

Final Report

Comprehensive Investigation of the Biogeochemical Factors Enhancing Microbially Generated Methane in Coal Beds

Project 07122-14

Colorado School of Mines, Golden CO
United States Geological Survey, Denver CO
University of Wyoming, Laramie WY

Dr. Junko Munakata-Marr
Principal Investigator
Email: junko@mines.edu

Colorado School of Mines
Golden, CO 80401

June 12, 2012

LEGAL NOTICE

This report was prepared by *Colorado School of Mines* and University of Wyoming as an account of work sponsored by the Research Partnership to Secure Energy for America, RPSEA. Neither RPSEA members of RPSEA, the National Energy Technology Laboratory, the U.S. Department of Energy, nor any person acting on behalf of any of the entities:

a. MAKES ANY WARRANTY OR REPRESENTATION, EXPRESS OR IMPLIED WITH RESPECT TO ACCURACY, COMPLETENESS, OR USEFULNESS OF THE INFORMATION CONTAINED IN THIS DOCUMENT, OR THAT THE USE OF ANY INFORMATION, APPARATUS, METHOD, OR PROCESS DISCLOSED IN THIS DOCUMENT MAY NOT INFRINGE PRIVATELY OWNED RIGHTS, OR

b. ASSUMES ANY LIABILITY WITH RESPECT TO THE USE OF, OR FOR ANY AND ALL DAMAGES RESULTING FROM THE USE OF, ANY INFORMATION, APPARATUS, METHOD, OR PROCESS DISCLOSED IN THIS DOCUMENT.

REFERENCE TO TRADE NAMES OR SPECIFIC COMMERCIAL PRODUCTS, COMMODITIES, OR SERVICES IN THIS REPORT DOES NOT REPRESENT OR CONSTIITUTE AND ENDORSEMENT, RECOMMENDATION, OR FAVORING BY RPSEA OR ITS CONTRACTORS OF THE SPECIFIC COMMERCIAL PRODUCT, COMMODITY, OR SERVICE.

LIST OF ACRONYMS

BSA: broad-spectrum analysis
CBM: coal bed methane
CH_4: methane
CO_2: carbon dioxide
CSM: Colorado School of Mines
DLI: direct liquid introduction
EI: electron ionization
ESI: electrospray ionization
ESTCP: Environmental Security Technology Certification Program
GC: gas chromatography
LC: liquid chromatography
MS: mass spectrometry
NSF: National Science Foundation
PEL: phosphoether lipids
PLFA: phospholipid fatty acids
SCF: standard cubic feet
SERDP: Strategic Environmental Research and Development Program
SPME: solid phase micro-extraction
SRB: sulfate-reducing bacteria
TCF: trillion cubic feet
USDA: United States Department of Agriculture
USGS: United States Geological Survey
UW: University of Wyoming

Comprehensive Investigation of the Biogeochemical Factors Enhancing Microbially Generated Methane in Coal Beds

Junko Munakata Marr, Principal Investigator (PI), Lee Landkamer, Kevin Mandernack and Linda Figueroa, co-PIs, Lisa Gallagher, Andy Glossner, Colorado School of Mines, Golden CO
Dave Bagley, Franco Basile and Michael Urynowicz, co-PIs, Zaixing Huang, Yiping Liu, Rajendra Mahat, Wesley Rodgers, University of Wyoming, Laramie WY
Steve Harris, co-PI, U.S. Geologic Survey, Denver CO

Research has shown that microorganisms are capable of converting coal to methane, though at widely different rates under controlled laboratory conditions. The methane is produced by methanogenesis, a process in which microorganisms (methanogenic archaea) convert substrates such as acetate or CO_2 and hydrogen into methane. The overall objective of this research was to systematically investigate processes involved in methanogenesis from coal to better understand how the process can be enhanced and accelerated. Project activities included characterizing the following factors that may lead to enhanced methanogenesis: (1) specific chemical constituents of coal, analyzed by methods such as gas chromatography and mass spectrometry, (2) specific microorganisms identified via phospholipid and DNA analyses, (3) culture growth amendments and conditions such as nutrient levels evaluated by microcosm CH_4 production, and (4) chemical pre-treatment of the coal with acids, bases, oxidants, solvents, and/or enzymes to release soluble organic matter that may subsequently stimulate the native microorganisms. Additionally, some of the dynamics of methanogenesis were captured in a computer model. All of these inquiries provide a broader understanding of microbial methane production from coal, as a critical first step to ultimately stimulating methanogenesis *in situ*.

Laboratory experiments have shown that the methane associated with coal can be increased from typical values of 60 SCF/ton to over 300 SCF/ton. As an example of the potential of enhanced methanogenesis, if 1% of the coal in the Powder River Basin could be converted to methane by adding inexpensive nutrients to stimulate existing microorganisms in the coal beds, approximately 30 TCF of gas would be produced, dramatically increasing reserves and profitability. In addition, if sufficient methane could be produced to exceed the solubility of methane in water, the gas could be produced without dewatering the coals, thus avoiding the costly dewatering step and its associated political and environmental complications.

A. Background

Methane can be produced from coal either thermogenically (abiotically) or biogenically. Thermogenic methane production occurs when buried organic matter is transformed at elevated temperatures and pressures (Rice and Claypool, 1981). Alternatively, methane generation can be driven by microbial activities. Conservative estimates indicate that 20% of the methane on the planet is the result of microbially catalyzed degradative processes (Rice and Claypool, 1981). Secondary biogenic methane production occurs when organic matter that was once deeply buried and transformed into coal has subsequently undergone uplift and cooling, making biogenic methane production a favorable process (Faiz and Hendry, 2006). Indeed, secondary biogenic gas may account for 15–30% of the total gas contents of coal seams (Scott et al. 1994) and some coal seams such as those in the Powder River Basin contain primarily biogenic gas (Rice, 1993).

The idea that microbes can metabolize coal has existed since the early 20th century (Potter, 1908), and microbes endemic to coal were first described several decades later (Rogoff, 1962). Nevertheless, these observations were not pursued further until more recent studies demonstrated the ability of bacteria and fungi to degrade coal in the laboratory, producing black, oily droplets that were visible in the growth medium (Cohen and Gabriele, 1982; Fakoussa, 1981). To date, several additional researchers have reported the ability of naturally occurring microorganisms and enzyme preparations to metabolize and solubilize coal (Faisson, 1991; Fakoussa and Hofrichter, 1999; Holker et al., 1999; Laborda et al., 1999; Catcheside and Ralph, 1999), but they did not address the prospect of methanogenesis. Indeed, the issue of methanogenic coal degradation has become a focus of applied research relatively recently (Volkwein et al., 1994; Shumkov et al., 1999). Relatively negative $\delta^{13}C$ values of methane ($\delta^{13}C_{CH4}$) have suggested that methanogenic archaea residing in coals naturally augment the production of CBM (Law et al., 1991; Smith et al., 1996; Aravena et al., 2003; Faiz et al., 2006; Strapoc et al., 2007), and there is growing interest in strategies for enhancing biogenic methane production in these deposits (Panow et al., 1997; Catcheside and Ralph, 1999; Ivanov, 2007). However, critical, peer reviewed work on direct analyses of the microbial populations and mechanisms of biogenic methanogenesis in coal deposits are lacking.

Figure 1 illustrates the general process of organic matter degradation under methanogenic conditions. This process occurs in multiple discrete stages and requires the concerted activities of several metabolically diverse groups of microorganisms (McInerney and Bryant, 1981). The initial reaction is likely a hydrolytic depolymerization of the parent organic material (Figure 1, Reaction 1) and is thought to be the rate-limiting step in the overall process (Boone, 1990). Lower molecular weight monomers are then further degraded via fermentative and syntrophic metabolism generating short-chain fatty acids, CO_2, and H_2 (Figure 1, Reaction 2). These intermediates (C_1 compounds and acetate) are rapidly consumed (Figure 1, Reactions 3 and 4) by methanogenic archaea leading to the production of methane.

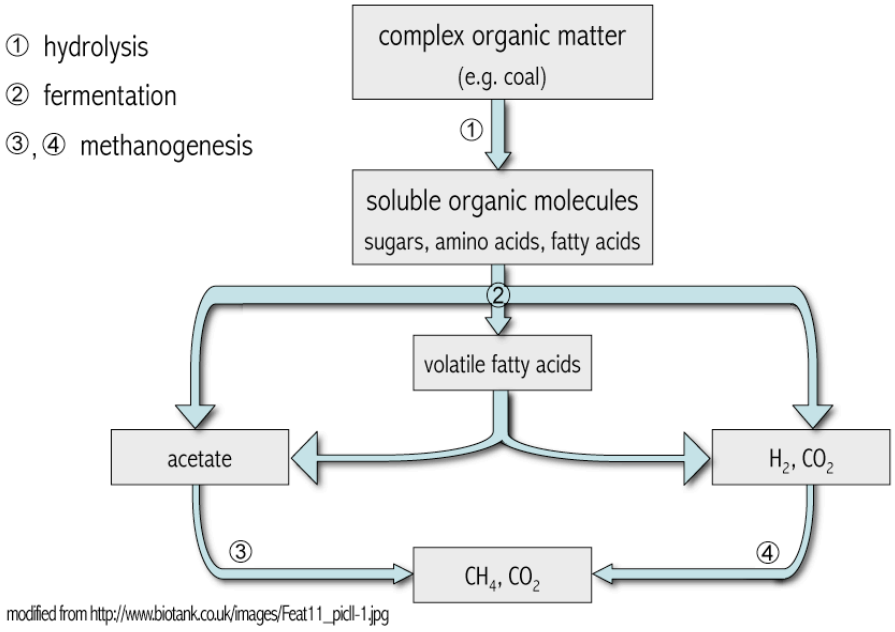

Figure 1. Simplified schematic illustrating the methanogenic degradation of organic matter. Circled numbers indicate the metabolic group of microbes involved in the particular stage of degradation. **1**: initial hydrolysis of polymeric carbon; **2**: fermentation of monomers to low molecular weight compounds; **3**: aceticlastic methanogenesis and **4**: CO_2-reducing methanogenesis from fermentation intermediates.

Stable isotope analysis of gas samples has proven to be a useful tool in delineating the source of methane in subsurface habitats (Whiticar, 1986) and implicates microbial methanogenesis as the likely mechanism by which natural gas is produced in many coalbeds worldwide (Scott, 1994; Smith and Pallasser, 1996; Clayton, 1998; Ahmed and Smith, 2001; Faiz and Hendry, 2006). In general, biogenic sources of methane have characteristically low δ13C values (eg., -100 ‰) and thermogenic sources higher values (~-40 ‰) (Whiticar et al., 1986). Hydrogen isotopic signatures of CH_4 of -333‰ and -227‰ generally reflect aceticlastic (Figure 1, Reaction 3) and CO_2-reducing (Figure 1, Reaction 4) pathways of methanogensis, respectively (Smith & Pallasser, 1996). Isotopic analyses of CBM suggest that different methanogenic pathways dominate in different coal beds (e.g., CO_2 reduction in Sydney Basin (Smith and Pallasser, 1996), aceticlastic in parts of the Powder River Basin (Rice, 1993)). However, the reasons for the differences in the methanogenic pathways in the different basins are unknown, though different coal ranks and water chemistry have been suggested as factors (Faiz and Hendry, 2006).

Preliminary experiments performed at the University of Wyoming with Powder River Basin coal have shown that various treatment methods (chemical oxidants or surfactants) can solubilize a fraction of the coal, significantly increasing the amount of dissolved organic carbon. These data suggest that a reservoir

of smaller molecular weight organic compounds exist within coal deposits and that these compounds can be released and made available to microorganisms using relatively passive *in-situ* treatment methods. The results of these studies are encouraging, however, additional research is needed to develop techniques to enhance the depolymerization and solubilization of coal into substrates that specifically enhance biogenic methane production.

The purpose of this project was to investigate the biotic and abiotic factors that influence bacterial degradation of coal in order to assess the potential for stimulating microbial methane production *in situ*, thereby providing a long-term domestic energy resource. This work characterized the methane-generating potential of coal in response to nutrient additions, chemical pretreatments of the coal and/or environmental manipulations in microcosm studies. Identifying the microbial communities and the microbial metabolic products formed en route to methanogenesis provides a broader understanding of microbial methane production in coal beds as well as strategies for stimulating methanogenesis *in situ*.

In summary, published studies of microbial methanogenesis from coal are few, and many studies lacked appropriate controls resulting in mixed results. The enormous potential of this microbial activity to generate such a valuable resource highlights the need for additional studies to substantiate whether this approach is truly viable. Specifically, this effort undertook carefully controlled laboratory experiments to identify the influential factors of methanogenesis from coal. These results will be critical to any effort designed to stimulate methanogenesis in the field. As such, this work represents a broad, concerted effort to rigorously document conditions under which modern biogenic methane production from coal can be enhanced. This work identified microbial consortia, coals, and environmental conditions that led to increased rates of gas production, such that these can be targeted in subsequent larger-scale feasibility studies.

I. OBJECTIVES

The following project objectives were pursued:

1. Identify chemical constituents of coal that are bioconverted.
2. Identify organisms within microbial consortia associated with biogas generation from coal.
3. Characterize the influence of culture growth amendments and conditions on biogas generation.
4. Determine coal pre-treatment impacts on levels of biogas precursor compounds, microbial communities, and ultimate methane generation.
5. Determine the rate limiting step(s) of microbial methane generation from coal.
6. Capture chemical and microbial dynamics observed in a computer model, to allow comparisons of different incubation scenarios.

II. RESULTS

The specific activities required to achieve the project objectives were divided into tasks. Results are detailed below.

Task 4.0—Sample Collection

Objective: The primary objective of Task 4.0 was to collect coal and groundwater samples from a variety of sites.

Several sampling trips were taken during the fall of 2008 and summer 2009. The first trip was taken to the Powder River Basin to obtain coal samples from freshly drilled wells completed near the time of sampling. These wells, sampled in November 2008, were drilled by Coleman Oil and Gas. Coal cuttings were obtained by straining them from the drill rig effluent and rinsing with sterile deionized water and purged with nitrogen in a sterile container, then stored at 4˚C until utilization. The second sampling trip was taken in April 2009 to Durango, CO to sample coal from the San Juan Basin. Coal was collected from outcrops near Durango as well as from a CBM well being drilled by BP. A return trip to the Powder River Basin was completed during September 2009 to sample wells being drilled by Anadarko Petroleum Corp. The coal collected during this trip was primarily from the Big George seam, but samples were also collected from the Smith and Wyodak seams as well. Coal collected during this trip became the primary substrate for subsequent experiments as it was the most abundant and productive of the samples collected. A sampling trip was also conducted in April 2010 to Trinidad, CO to sample from the Raton Basin. Due to difficulties with drilling this particular well, only a small mass of coal was collected at this time.

Task 5.0—Coal Pretreatment

Objective: This task evaluated methods designed to enhance coal solubility to address project objective 4.

5.1 Soluble organic carbon

Our previous studies (data not published) indicated that the particle size of coal, treatment duration, chemical concentration and pH environment of the coal and water mixture prior to addition of chemical agents had impacts on the solubilization/depolymerization. The yield of total organic carbon (TOC) is usually higher for the use of small particle size, higher treatment concentration and longer treatment duration. Low and high treatment concentrations of chemicals with coal particle smaller than 0.25 mm were chosen to treat for four months. Because pH tends to have profound impacts on coal solubility, pH was eliminated as a variable.

Figure 1 shows the soluble carbon profile of different pre-treatment methods applied to coal from the Powder River Basin, Upper Wyodak formation. Total organic carbon (TOC) and non-purgeable carbon (NPOC) were directly measured by TOC analyzer (Shimadzu), with purgeable organic carbon (POC) calculated as the difference of TOC and NPOC. For the analysis of NPOC, the sample was acidified to pH 2 with 2 M HCl solution and sparged with zero grade air gas for 1.5 min automatically by the TOC analyzer.

The nitric acid at high treatment concentration (NA-C3) generated the highest soluble carbons for both TOC and NPOC. The concentrations were as high as 3038 and 2832 mg/l for TOC and NPOC, respectively. For NA-C3, 14.0% of the carbon of coal was solubilized. The sodium hydroxide at low treatment concentration (SH-C1) generated the second highest TOC (1521 mg/l) and NPOC (1317 mg/l) contents. Potassium permanganate at high concentration yielded the next highest TOC (PP-C3, 1144 mg/l), followed by sodium hydroxide at high concentration (SH-C3, 928 mg/l), nitric acid at low concentration (NA-C1, 236 mg/l), and potassium permanganate at low concentration (PP-C1, 224 mg/l). Sodium hydroxide at high concentration (SH-C3, 715 mg/l) had the third highest NPOC, followed by PP-C3 (597 mg/l), NA-C1 (186 mg/l) and potassium permanganate at low concentration (PP-C1, 115 mg/l). With respect to POC, the PP-C3 had the highest yield at 574 mg/l and followed by SH-C3 (213 mg/l), NA-C3 (206 mg/l), SH-C1 (205 mg/l), PP-C1 (112 mg/l) and NA-C1 (50 mg/l). Hydrogen peroxide treatments generated the lowest TOC, NPOC and POC regardless of the concentration of the treatment agent.

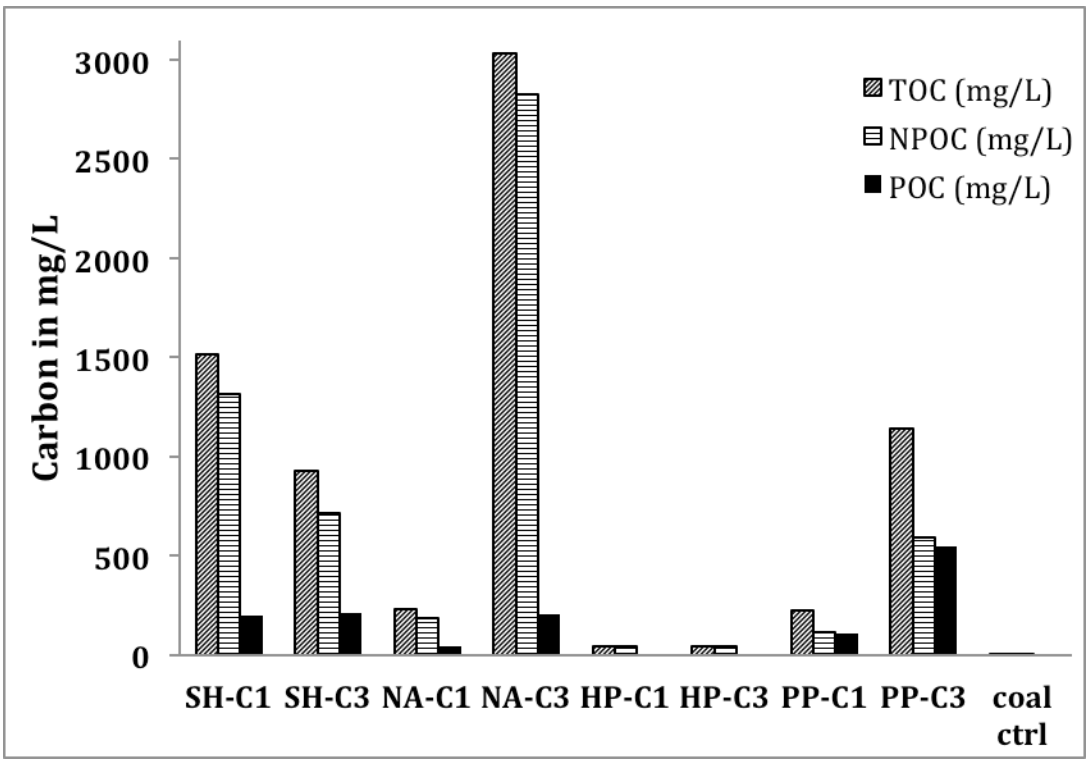

Figure 1. Concentration of soluble organic carbon, TOC: total organic carbon, NPOC: non-purgable organic carbon, POC: purgable organic carbon; SH: sodium hydroxide, NA: nitric acid, HP: hydrogen peroxide (catalyzed), PP: potassium permanganate, coal ctrl: coal and water mixture controls; C1: low concentration, C3: high concentration. Data points represent means of three replicates.

In addition, Big George coal was treated with different amounts of HNO_3 and NaOH. The NPOC results of the nitric acid extraction are summarized in Table 1. The NPOC concentration increased with decreasing coal/nitric acid mass ratio, indicating that more nitric acid facilitated greater solubilization of un-oxidized coal. VFAs and alcohols analysis indicated that acetic acid and unidentified alcohols were produced by HNO_3 treatment, and the concentrations of the acetic acid and an unidentified alcohol (retention time of 2.7 min) increased with increasing the amount of nitric acid (Table 2).

Table 1. NPOC Concentration from HNO_3 Treatment of Big George Coal

Coal /Nitric acid, g/g	NPOC, mg/L (mean±range)
1:0	5.5±0.2
1:0.2	6.2±0
1:1	27±0.7
1:2.5	294±38
1:5	656±0.1 (1176±87)[a]

[a] Coal was treated in different batch.

Table 2. VFAs and Alcohols Analysis of Filtrate from HNO_3 Treated Big George Coal

Compounds	Retention Time, minutes	Peak Area		
		Coal/HNO_3, g/g		
		1:1	1:2.5	1:5
Compound 1	1.81	1598±1556	ND[a]	ND
Compound 2	2.61	7266±1740	1170±858	4635±563
Compound 3	2.69	970±83	9124±4045	23731±1611
Compound 4	3.51	1636±905	546±303	1049±77
Acetic acid	4.60	ND	74±25[b]	145±58 [c]

[a] ND= Not detected
[b] The concentration of acetic acid is 135±14 mg/L
[c] The concentration of acetic acid is 145±58 mg/L

The NPOC analysis results of sodium hydroxide treatment are summarized in Table 3. The NPOC concentration increased with decreasing coal/sodium hydroxide mass ratio to 1:0.64, and then decreased with further decreases the coal/sodium hydroxide mass ratio. A precipitate was formed when hydrochloric acid was used to adjust the pH of the filtrate to 7.0. Additionally, when the extract was processed through a cation exchange system to remove Na^+, the concentration of NPOC decreased (Table 3). Interestingly, the NPOC after cation exchange treatment consistently increased as the coal/sodium hydroxide mass ratio was decreased.

Table 3. NPOC Concentration of NaOH Extraction from Big George Coal

Coal /NaOH, g/g	NPOC, mg/L	
	Before cation ion exchange resin treatment	After cation ion exchange resin treatment
1:0	5.5±0.2	N.D.[1]
1:0.12	54±2	48±6
1:0.64	472±23	94±2
1:1.6	411±3	170±20
1:3.2	178±8	184±12

[1]ND=Not detected

The analysis for VFAs and alcohols indicated that the concentration of an unidentified alcohol (retention time of 2.43 min) increased with increasing the amount of NaOH from 0 to 0.64 g (Table 4).

Table 4. VFAs and Alcohols Analysis of Filtrate from NaOH Treated Big George Coal

	Retention Time, minutes	Peak Area	
		Coal/NaOH, g/g	
		1:0.12	1:0.64
Compound	2.43	1842±168	30841±2038

[1] Peak area was adjusted using international standard.
[2] Did not include results of per gram coal treated with 1.6 g or 3.2 g NaOH because the strong base affected analysis method.

5.2 3D-EEM

The fluorescence of organics is due to the presence of fluorophores that absorb photons, followed by excitation to a higher electronic energy state. Then the absorbed energy is released to the environment at a greater wavelength (McKnight et al., 2001; Amy and Drewes, 2006). Fluorescence spectrometry can be used to distinguish humic-like and fulvic acid-like organic matter from protein-like organic matter for natural organic matter or aromatic compound for coals (Jaffrennou et al., 2007). Amy and Drewes (2006) quantified the fluorescence intensity for protein-like organic matter at an emission wavelength of 330 nm and an excitation wavelength of 270 nm. Humic- and fulvic acid-like intensities were quantified at emission wavelengths of 420 and 440 nm and at excitation wavelengths of 330 and 240 nm, respectively. Aromatic compounds with 1 and 2 rings are located at emission wavelengths from 300 to 350 nm and at excitation wavelengths from 280 to 330 nm while for PAHs with 3 to 5 rings, the spectra show at emission wavelengths from 370 to 480 nm and at excitation wavelengths from 360 to 460 nm (Jaffrennou et al., 2007). The samples resulting from the chemical treatments had humic-like, fulvic-like peaks and aromatic/PAHs region instead of protein-like peak, as shown in Figure 2. The Em/Ex (emission/excitation) wavelengths of the peaks are shown in Table 5.

Sodium hydroxide: For sodium hydroxide treatments (Figure 2, A & B), humic-like, fulvic-like and aromatic/PAHs organic matter were observed in the spectra. The oblique bar on the upper left corner was the aromatic/PAHs compounds for both low and high treatment concentrations. The fluorescence intensity was higher for the low treatment concentration. For low concentration treatment, the Em/Ex wavelength couples occurred at 462/252.5 nm and 470/362.5 nm for fulvic-like and humic-like peaks, respectively. The counterparts of high concentration treatment occurred at 430/232.5 nm and 426/312.5 nm, respectively. The fluorescence intensity is higher for the high concentration treatment for both fulvic-like and humic-like peaks.

Nitric acid: Similar to the NaOH treatment, the fluorescent spectra of nitric acid treated samples showed fulvic-like, humic-like and aromatic/PAHs peaks (Figure 2, C & D). The aromatic/PAHs bar of low concentration treatment extended to lower Em/Ex wavelengths while for high concentration treatment, the aromatic/PAHs region limited to higher Em/Ex wavelengths. The low concentration treatment samples have higher fluorescence intensity of aromatic/PAHs region. For low concentration treatment, the Em/Ex (emission/excitation) wavelength couples occurred at 426/250 nm and 422/315 nm for fulvic-like and humic-like peaks, respectively. The counterparts of high concentration treatment occurred at 450/265 nm and 434/337.5 nm. The fluorescence intensity is higher for the high concentration treatment for both fulvic-like and humic-like peaks.

Catalyzed hydrogen peroxide: The catalyzed hydrogen peroxide treated samples showed aromatic/PAHs peaks at higher Em/Ex wavelengths (Figure 2, E & F). The fluorescence intensity was

higher for low concentration treatments. There was no fulvic-like or humic-like peak for both of the treatment concentrations.

Potassium permanganate: All three types of peaks including fulvic-like, humic-like and aromatic/PAHs were identified in the spectra (Figure 2, G & H). The aromatic/PAHs peak extended from low to high Em/Ex for both concentrations of treatment, only that the fluorescence intensity was slightly higher for low concentration treatment. For low concentration treatment, the Em/Ex (emission/excitation) wavelength couples occurred at 430/215 nm and 426/315 nm for fulvic-like and humic-like peaks, respectively. The counterparts of high concentration treatment occurred at 426/232.5 nm and 426/312.5 nm. The fluorescence intensity is much higher for the high concentration treatment for both fulvic-like and humic-like peaks.

Table 5. The Em/Ex wavelengths of the humic- and fulvic-like peaks

	SH-C1		**SH-C3**		**NA-C1**		**NA-C3**	
nm	HLP	FLP	HLP	FLP	HLP	FLP	HLP	FLP
Em	470	462	426	430	422	426	434	450
Ex	362.5	252.5	312.5	232.5	315	250	337.5	265
	HP-C1		**HP-C3**		**PP-C1**		**PP-C3**	
nm	HLP	FLP	HLP	FLP	HLP	FLP	HLP	FLP
Em	--	--	--	--	426	430	426	426
Ex	--	--	--	--	315	215	312.5	232.5

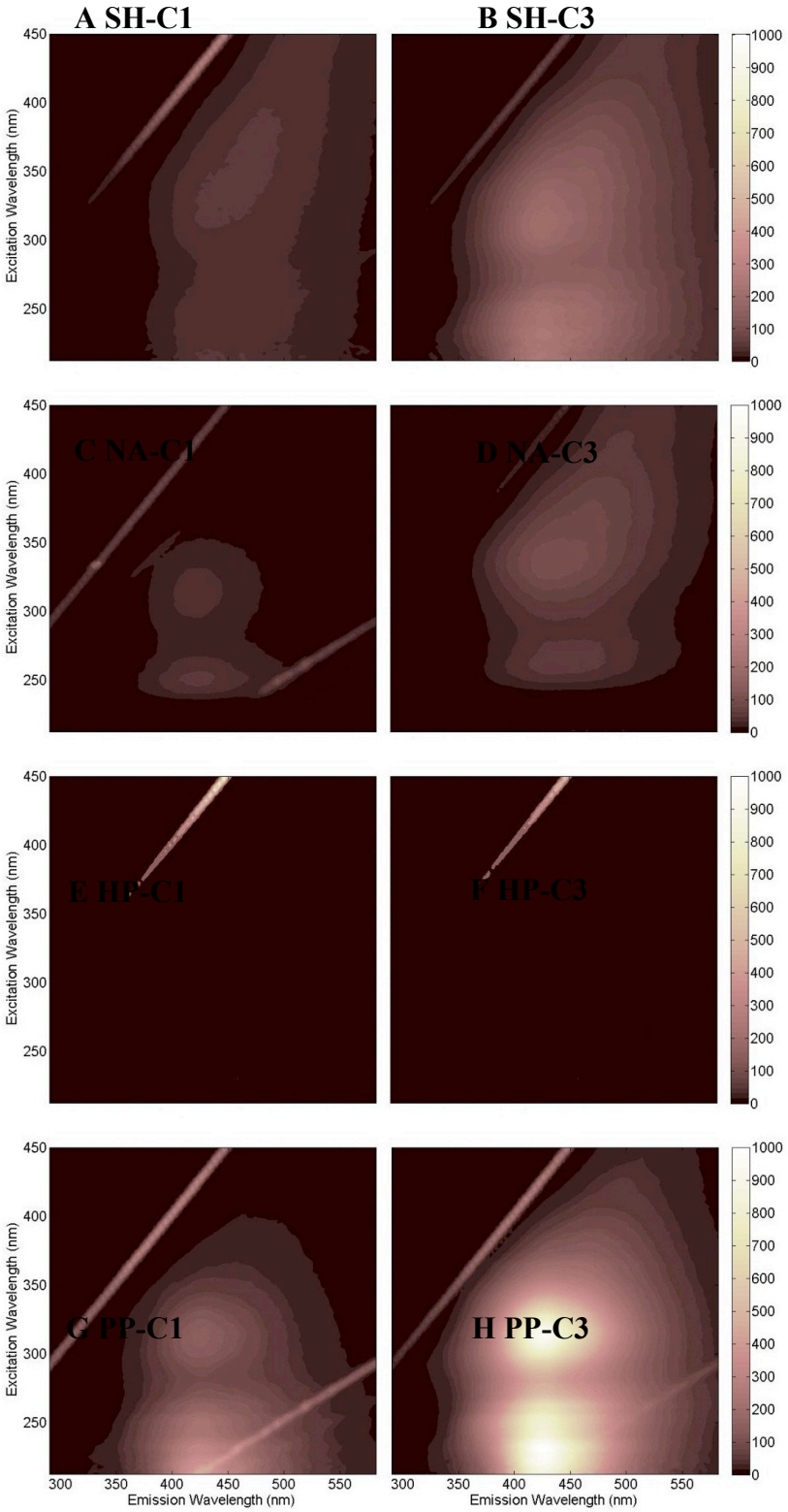

Figure 2. 3-D Fluorescence Spectra: Emission Excitation Matrix (EEM) A: Sodium hydroxide low conc.; B: Sodium hydroxide high conc.; C: Nitric acid low conc.; D: Nitric acid high conc.; E: Catalyzed hydrogen peroxide low conc.; F: Catalyzed hydrogen peroxide high conc.; G: Potassium permanganate low conc.; H: Potassium permanganate high conc. Spectra represent means of three replicates.

5.3 Respirometric study

Figure 3 shows the CO_2 evolution for different treatment agents during a period of 14 days. The amount of CO_2 produced for each of the liquid samples was normalized to per gram coal. Apparently the coal pretreated with high concentration (0.1 M) of permanganate produced significant higher concentration of CO_2 than others. About 1.1% (0.57 mmol/ g coal) of the carbon from original coal was bioconverted to carbon dioxide at 14-day, followed by SH-C1 (0.5%), SH-C3 and NA-C1 (0.3%), PP-C1 and NA-C3 (0.2%). However, calculated the ratio of soluble carbon used for producing CO_2, up to 25.8% of the soluble carbon was bioconverted for NA-C1 within 14 days, followed by PP-C1 (21.9%), PP-C3 (20.0%), SH-C1 (7.1%), SH-C3 (6.7%) and NA-C3 (1.1%).

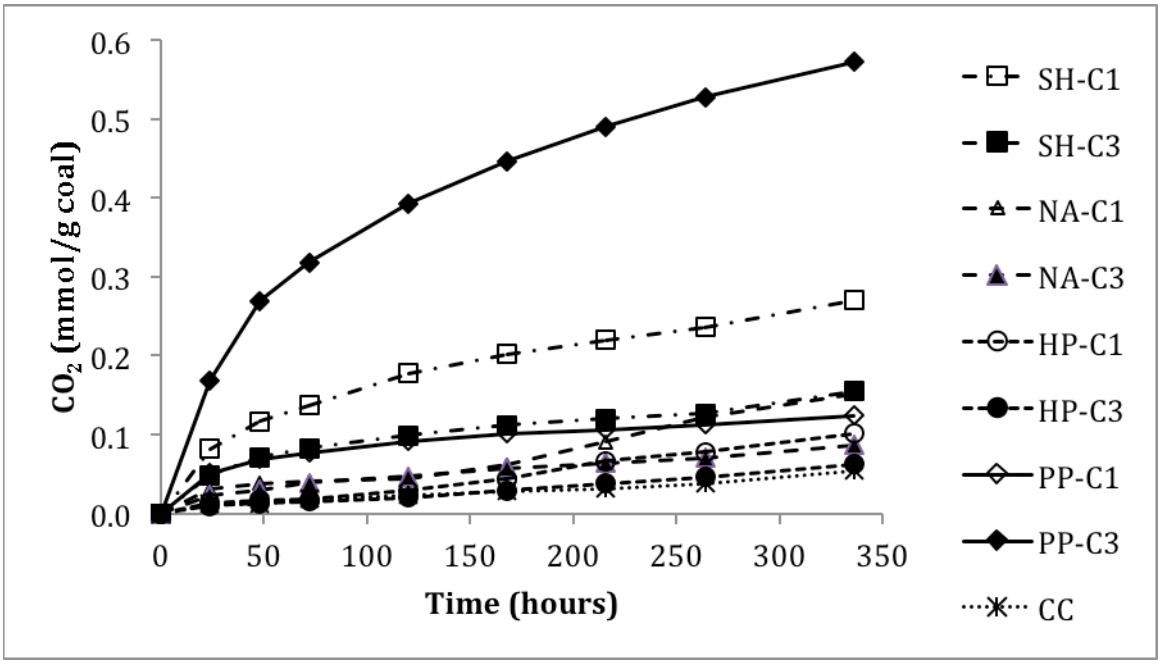

Figure 3. Cumulative CO_2 productions in biometer experiment for treated liquid samples. SH=sodium hydroxide NA=nitric acid HP=hydrogen peroxide PP=potassium permanganate, CC=coal and water mixture controls, WC=water only control; C1=low concentration C3=high concentration. Data points represent means of three replicates.

Task 6.0 - Chemical Characterization of Different Coals, Pre-treated Coals and Associated Waters.

Objective: This task characterized the soluble organic matter derived from coal that is potentially bioavailable. In combination with Task 7, this task addresses project objective 1.

Due to the broad spectrum nature of the analysis of coal samples, sample preparation is critical as it must sample molecules with a wide range of physicochemical properties of molecular mass, polarity and reactivity. Because of this extensively complex range of molecular properties of the "target" analytes, the possibility of bias during the sample preparation step is often inevitable and most often un-testable due to

the lack of knowledge about the composition of the sample. As a result, sample preparation steps geared towards a broad spectrum analysis often rely on several parallel or serial extraction steps that bracket the wide range spectrum of molecular properties. This strategy can be effective when the sample extraction protocol is rapid; however, it becomes impractical when a single preparation protocol involves an extraction step of 24 hours or more.

Soxhlet extraction has been traditionally used for the extraction of complex samples like coal. However, current standard procedures require an average of 72 hours of heating. This sample preparation turnaround time is not amenable for routine analysis of coal samples by GC-MS. As part of this RPSEA-funded project, faster approaches for the analysis of coal samples were developed. The first method developed is based on either microwave radiation heating or convection oven heating of the coal sample in a suitable solvent in a pressurized vessel. The sample extraction time was reduced to 4 hours and reducing the cost and complexity of the extraction (*i.e.*, does not use special glassware). The second method of analysis is based on the analysis of coal samples in its native state by Direct Insertion Probe-MS.

Extraction of analytes from solid samples has typically been carried out by a Soxhlet extraction apparatus with a solvent of choice. This method extracts all volatile matter from the sample while leaving behind a solid matrix. For coal samples, this extraction process typically takes around 72 hours to complete, but is the most consistent and most thorough extraction process available.[3] Soxhlet extraction apparatuses (Figure 4) are available in different sizes depending on the sample to be extracted and the amount of extract needed.

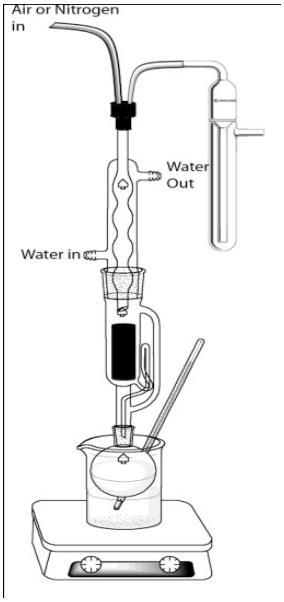

Figure 4. Soxhlet extraction apparatus setup where air in is either nitrogen or compressed air and the complete closed system with a bubbler for air evacuation.

Coal from multiple sources is often analyzed and compared using Soxhlet apparatuses; the results from such tests are most useful if extractions are analyzed within the same time period. Multiple Soxhlet apparatuses are needed, so coal extracts can be analyzed consecutively in order to compare different coal samples. This strategy either costs extra money upfront to buy several Soxhlet apparatuses or it would take weeks of sequential extractions to get all extracts needed for a proper comparison. A faster way to prepare coal extract is using a combination of heat and pressure in a sealed vial. This can be completed by one of three different ways: 1) heating a sealed vial in an oil/water bath, 2) heating a sealed vial in an oven, or 3) heating a sealed vial in a microwave. The first two methods are indirect heating, while the third way is direct heating. An oil bath and an oven are considered indirect heat, because the sample (in this case coal) is being heated by the solvent. On the other hand a microwave heats the sample directly along with the solvent used and therefore is considered direct heat. In this section, results are shown where each of these methods is compared with Soxhlet extraction. For proper comparison, each extraction trial is kept at a 1:5 ratio of coal to solvent. This ratio keeps the relative abundance of volatile matter in the coal extract constant and gives the best possible results. Each extract is also condensed down to 5% volume of the original extraction solvent prior to GCMS analysis.

Using a research grade microwave and a vial with a crimp top and polytetrafluoroethylene (PTFE) septa to seal the system so no solvent or analyte is lost, a faster extraction is achieved. The direct heat from the microwave causes the coal to heat up faster and to a hotter temperature, making the extraction process faster without the loss of volatile matter. The time for a microwave system to heat the sample, under these conditions (pressurized tube), cuts down the extraction time to 4 hours, a 94% reduction in extraction time. The total volume of extract and solvent in the Soxhlet system is normally around 100 mL total volume, whereas the microwave system uses only about 5 mL total volume. Using the Soxhlet extraction procedure, each coal extraction takes three and a half days to complete, so the analysis of multiple coal samples extractions must be performed sequentially, which takes many days to complete. Since it is a known method, the Soxhlet extraction was chosen to set a baseline for sample preparation and is compare to all the new developed methods for coal extraction. Analysis of the extracted samples was performed by GC-MS.

Analysis of the soxhlet coal extract from Durango coal resulted in a complex chromatogram (Figure 5). To get more information from the analysis of coal, the coal extract was fractionated prior to GC-MS. Each fraction is collected, dried, and resuspended in 1 mL hexane for further analysis by GCMS.

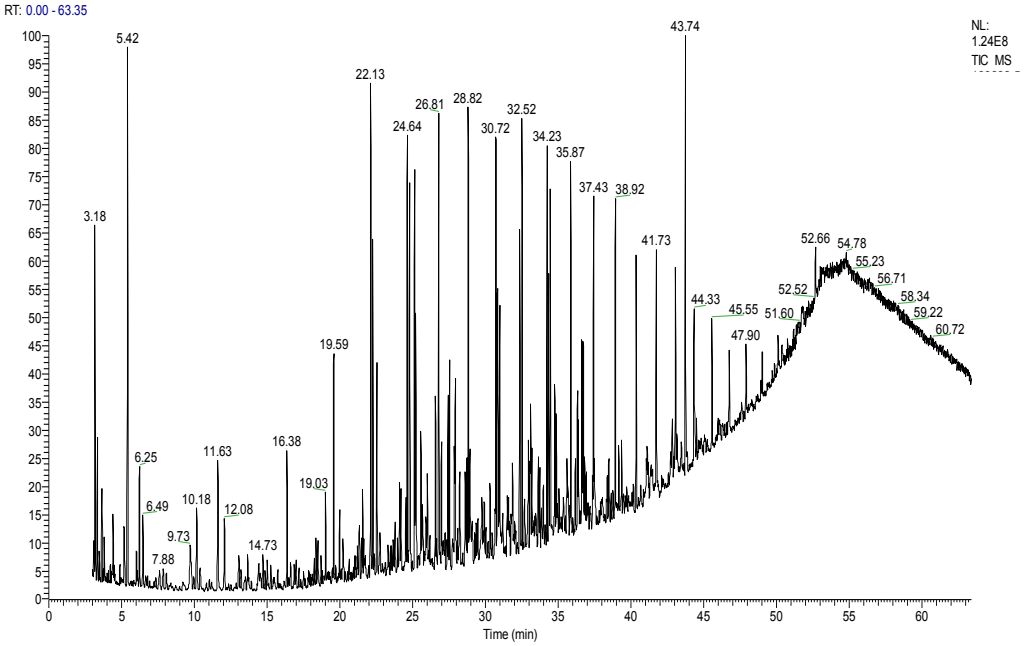

Figure 5. Durango outcrop coal anaerobic extract chromatogram. Many peaks clustered together making analysis harder. Further separation or knowledge of likely compounds needed for analysis.

The fractionation process results in different fractions of compound classes: particularly alkanes, hopanes, alkylated naphthalenes, and phenanthrenes (see Figure 6 for representative structures for each class of compound). Analysis of these fractions with the GC-MS gives an idea of the composition of the coal sample. AMDIS analysis results (Appendix 1) show many hydrocarbon chains being extracted in proposed lengths of up to 27 carbons (heptacosane). To facilitate the analysis of GC-MS data, characteristic ion signals for each class of compounds are used to construct extracted ion chromatograms (XIC). For example, for alkanes, m/z 57 is a characteristic ion regardless of the molecular mass of the parent molecule, all alkanes fragment under EI conditions to produce this ion. This is equal for hopanes m/z 191; for alkylated naphthalenes m/z 128, 156, 170, and 184; and for alkylated phenanthrenes m/z 178, 192, 206, 220, and 234.

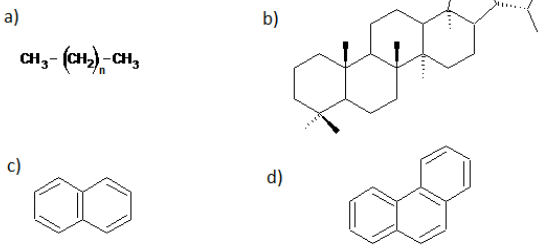

Figure 6. Base structures of a) alkanes, b) hopanes, c) naphthalenes, and d) phenanthrenes.

The retention time in GC of alkyl chain hydrocarbons are evenly spaced (for temperature programmed GC) as they increase in the number of -CH_2 groups, which in turn increases the boiling point of the compound. Each analysis completed on the GC-MS instrument was completed in sequence of each other with a blank and standard solution analysis intermixed in the sequence. Analysis in this procedure ensures

proper comparison of data to be viable. Figure 7 shows the chromatogram of the first two fractions, leaving fraction 3, the polar fraction, for future analyses. Using functions built into the Xcalibur software, XIC's for each compound class was looked at individually and analyzed using the NIST 2.0 database search.

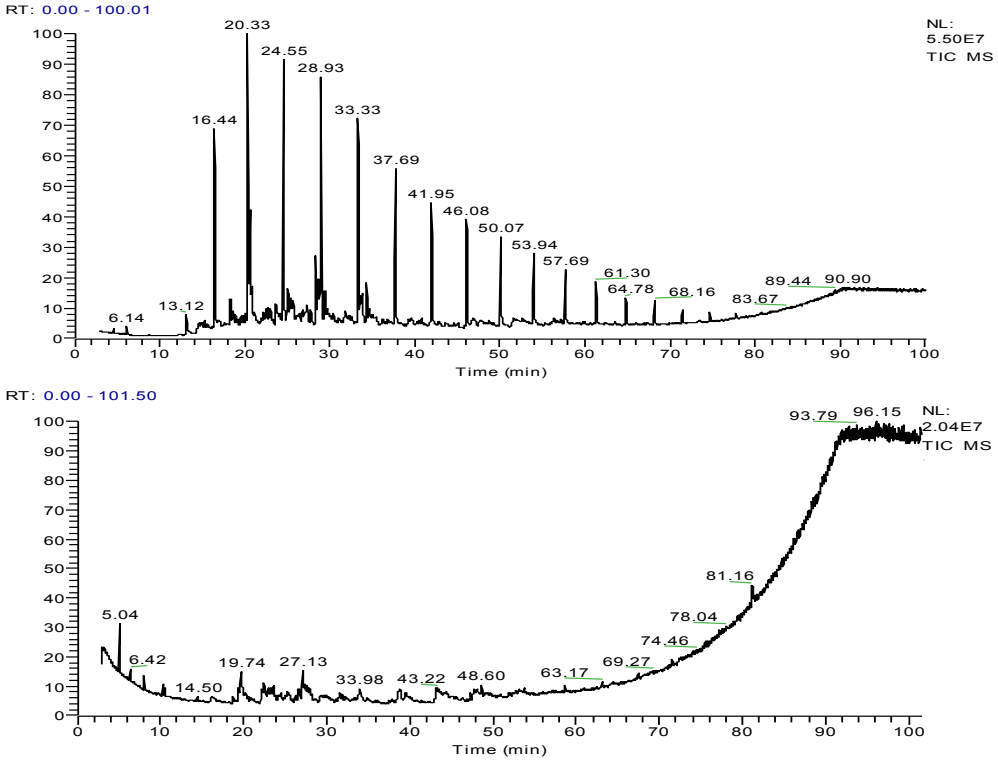

Figure 7. Chromatograms of Fraction 1 aliphatic compounds (top) and Fraction 2 aromatic compounds (bottom) from column fractionated Durango outcrop coal extract.

After each fractionation, a layer of black matter is left on the top of the gravity column that is not soluble in chloroform, dichloromethane, hexane, or methanol. To avoid possible cross contamination of products, the column material was changed to fresh column packing after each separation. The added time and cost of separating each coal extract on a column did not prove to be time and cost effective so only selected samples were fractionated. Instead, the coal extract was analyzed by GC, which separates molecules mainly based on their boiling points and polarity before analysis by MS. Analysis done in this manner will show most of the peaks associated with an extract, with the exception of highly polar compounds or high molar mass/high-boiling point molecules. However chromatograms clustered with added peaks make for a higher probability of co-eluting compounds, making compound identification less reliable. A new temperature program to run on the GC oven was created with a slower temperature ramp to increase the selectivity and help resolve the peaks. The major advantage of analysis of entire coal extract is that all samples can be completed in less time with less sample preparation and less chance of compound

loss or human error. Figure 8 shows an XIC of each family of compounds for the Durango Outcrop coal extract. Looking at Figure 8a), many different lengths of hydrocarbon chains are apparent, XIC 57, with the largest proposed to be heptacosane [$CH_3(CH_2)_{25}CH_3$] as obtained from AMDIS analysis report.

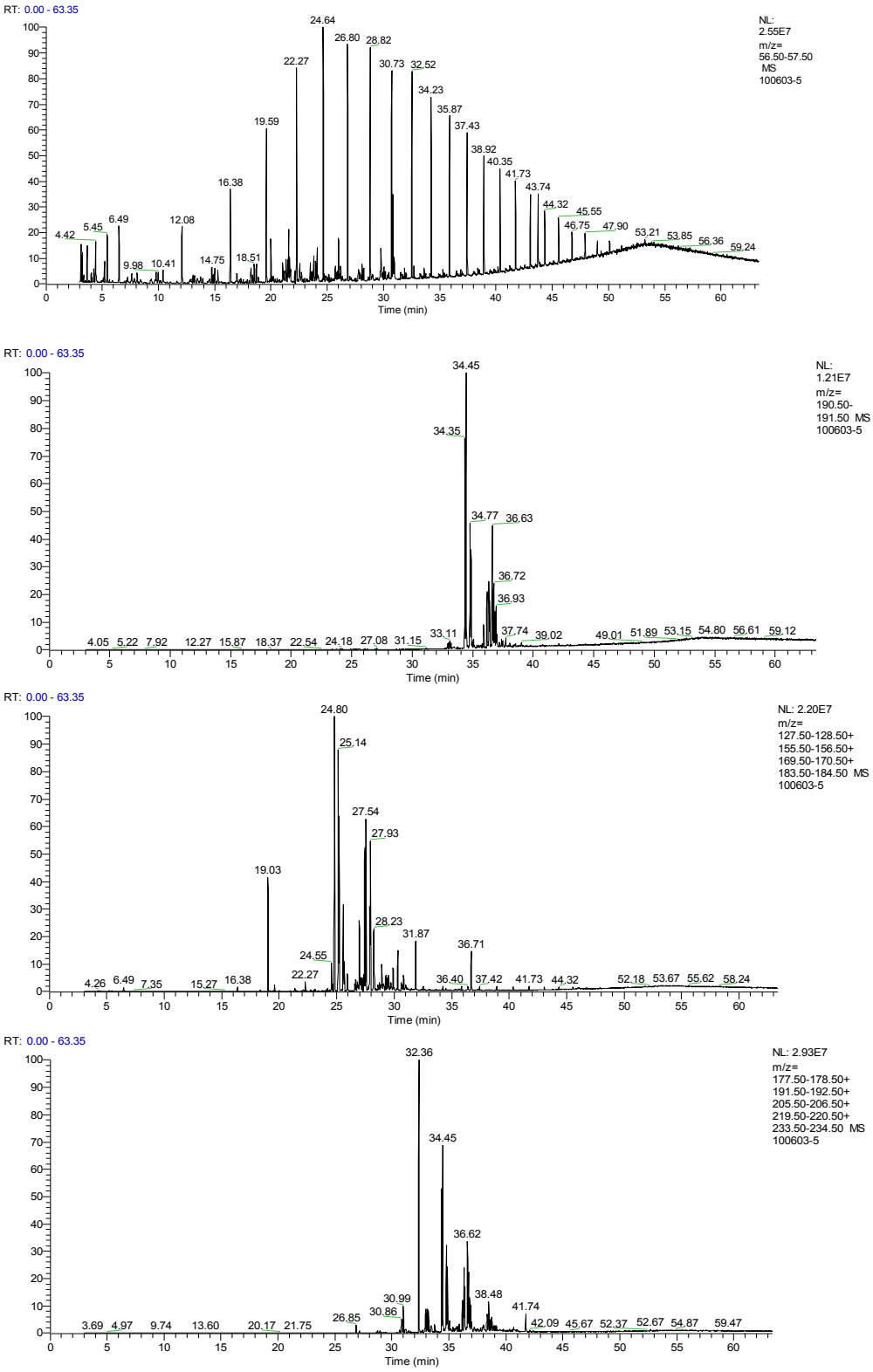

Figure 8. Extracted Ion Chromatograms (XIC) showing the different family of compounds, a) alkanes m/z 57, b) hopanes m/z 191, c) alkylated naphthalenes m/z 128, 156, 170, and 184, and d) alkylated phenanthrenes m/z 178, 192, 206, 220, and 234.

Extraction Technique Comparison. Microwave extracts and Soxhlet extracts were compared by GC-MS analysis to see similarities and differences in extraction processes. GC-MS analysis of coal extracts obtained from these different extraction techniques show that constant temperature in the microwave oven results in less concentrated extract when compared to a Soxhlet extract as determined by the intensity of the total ion count, TIC, signal in the chromatogram (Figure 9a). On the other hand, a microwave extraction performed at constant power showed similar concentration to that obtained by Soxhlet extraction (Figure 9b). These results lead to another question: is it the constant power from the microwave or is it the high temperature and high pressure helping extract organic matter from coal? To answer this question, microwave extraction was compared to an extraction of the coal in the same closed system glass tube being heated constantly by: 1) an oven (dry heat) and 2) an oil bath (wet heat). Both processes are closed systems using indirect heating of the coal. The solvent is heated by the oven or oil, helping decipher if the microwave irradiation extracts by heating the coal directly or heating the solvent causes increased pressure in the system.

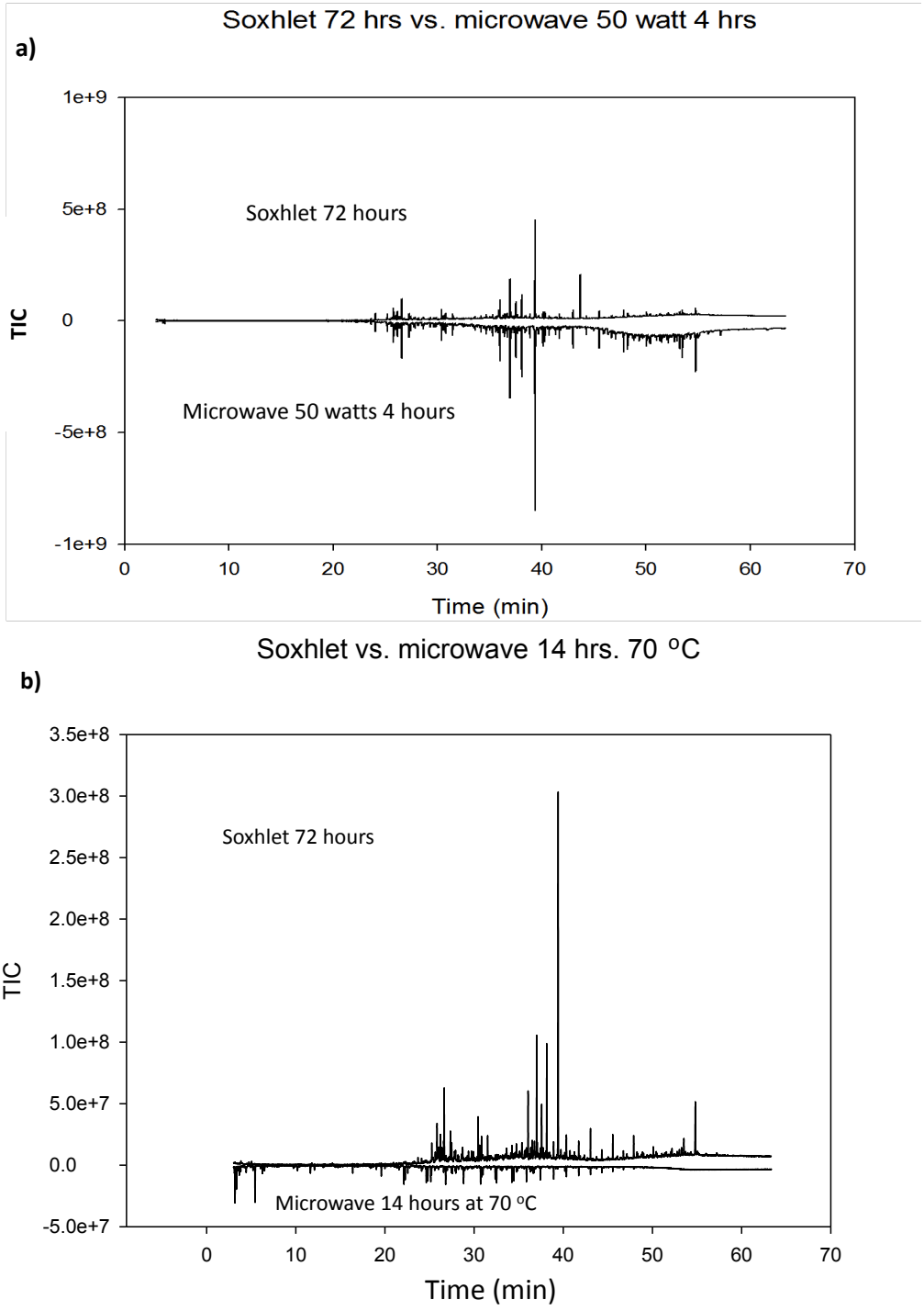

Figure 9. a) comparison of soxhlet 70°C 72 hours vs microwave using constant power 50 watts for 4 hours. The Soxhlet has less total relative abundance when comparing TIC. b) comparison of Soxhlet 70°C 72 hours vs. microwave using constant temperature 70° for 14 hours. Soxhlet has higher relative abundance when comparing TIC.

Using an oil bath on the closed system caused the septa in the vial to expand to a point of rupture and all extract was lost. Using the dry heat in the oven (a GC oven was used in this case, one not connected to a MS detector) made the vial septa expand slightly but never to a point of failure. GC-MS analysis of the oven heated extract was compared to the microwave extraction and the Soxhlet extraction (Figure 10). Chromatograms from all three extraction procedures showed similar trends, but the Soxhlet extract showed a less intense TIC compared to the microwave extract. The oven also showed a higher TIC than the Soxhlet extract, but less when compared to the microwave extract. AMDIS analysis (Appendix 1) of microwave and oven results detected an 86% match between the closest in peaks. Microwave and Soxhlet extractions are more similar in peaks detected than oven and soxhlet extractions at 80% to 76%, respectively.

These results demonstrate that extraction of volatile matter from coal can be achieved using a microwave or oven and a sealed vial if high pressure and temperature is achieved. Using chloroform as the extraction solvent, a temperature of 110°C, and pressure reaching around 150 psi, an oven or microwave extraction is statistically similar to a Soxhlet extraction and takes 94% less time, 4 hours compared to 72 hours. Faster extraction times and more controllable anaerobic conditions make using a microwave or oven and a sealed vial a viable alternative to a Soxhlet extraction apparatus.

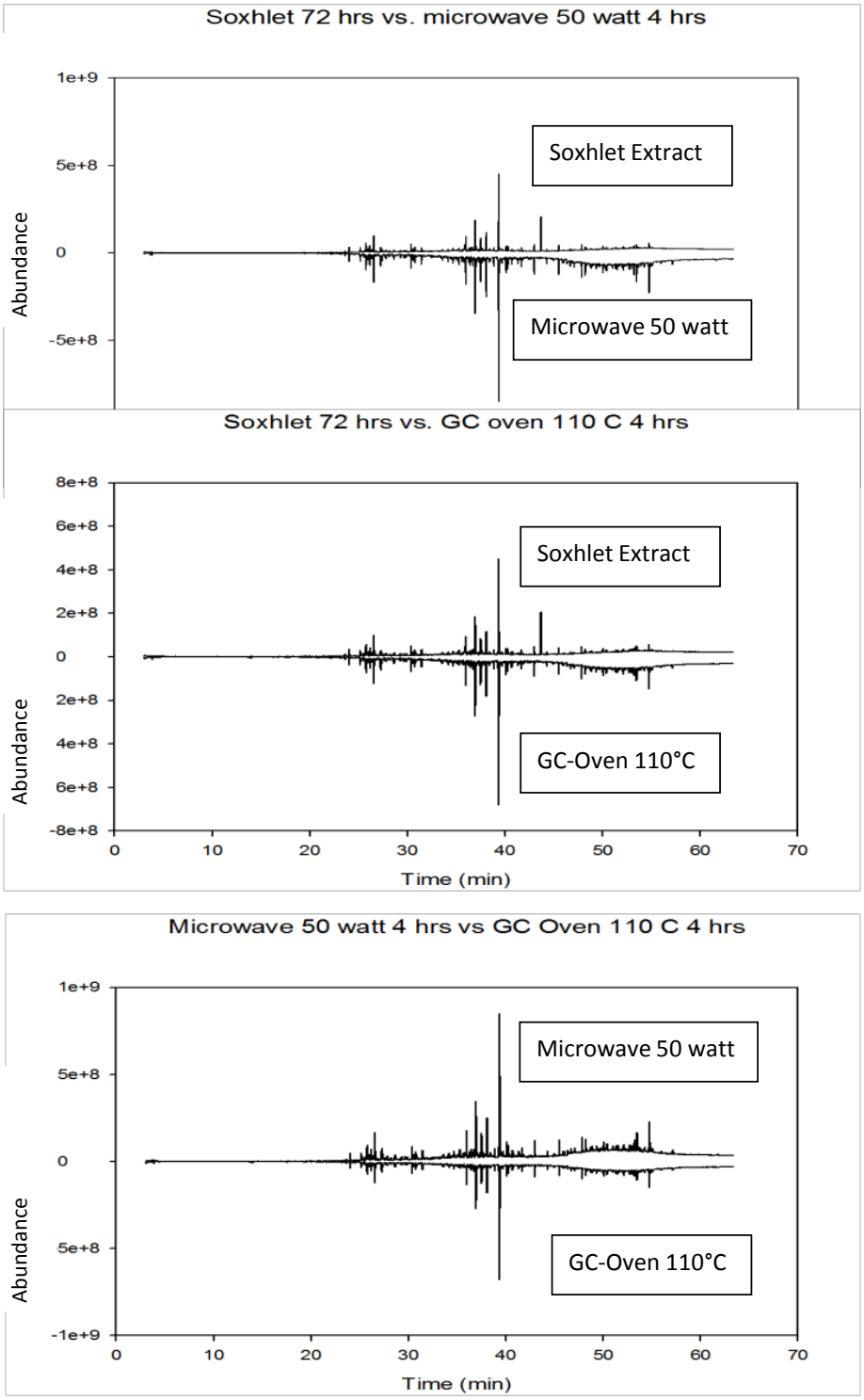

Figure 10. Comparison of Soxhlet extraction 72 hours, Microwave extraction 4 hours at 50 watts, and oven extraction 4 hours at 110°C.

Task 7.0—Microbial Enrichment and Characterization

Objective: This task consisted of several integrated efforts designed to better understand the metabolic pathways of microbial consortia involved in methane generation from coal. It also evaluated the effect of nutrients, environmental conditions and pre-treatments on methane generation. Microbes associated with native coal samples and produced waters were identified by a variety of methods, microbial cultures that generate methane from coal were enriched and characterized and coal biotransformation intermediates were identified. The task will address project objectives 1, 2, 3 and 4.

7.1: Microbial enrichment

Samples collected from various sampling trips were first screened for methane production utilizing the native microbes present on the coal. The medium used for growth was prepared following the procedures of Tanner (2006). The medium included (g/L) NaCl (0.8), NH_4Cl (1.0), KH_2PO_4 (0.1), KCl (0.1), $MgCl_2 \cdot 6H_2O$ (0.17), $CaCl_2 \cdot 2H_2O$ (0.04), $NaHCO_3$ (1.0), nitrilotriacetic acid (0.02), $MnSO_4 \cdot H_2O$ (0.01), $Fe(NH_4)2SO_4 \cdot 6H_2O$ (0.008), $CoCl_2 \cdot 6H_2O$ (0.002), $ZnSO_4 \cdot 7H_2O$ (0.002), $CuCl_2 \cdot 2H_2O$ (0.0002), $NiCl_2 \cdot 6H_2O$ (0.0002), $Na_2MoO_4 \cdot 2H_2O$ (0.0002), Na_2SeO_4 (0.0002), Na_2WO_4 (0.0002). The medium was prepared by flash-autoclaving DI water to reduce oxygen saturation, then sparging with 4:1 N_2:CO_2 for 15 minutes before adding 10 mL of Tanner's trace metal solution, 50 mL trace mineral solution, and 1 g/L $NaHCO_3$ just before sealing under N_2:CO_2 and autoclaving. Anaerobic trace vitamin solution was added according to Tanner (2006). Upon sealing with butyl rubber stoppers, the headspace of each bottle was purged with 4:1 N_2/CO_2 and pressurized to 110 kPa.

Initial experiments were designed to enrich for organisms already present on the coal without adding an external inoculum. The results of these first experiments are shown in Figure 11, which shows incubations with coal from various wells sampled during the September 2009 sampling. Subsamples of the most productive incubations from well 23-34 were then transferred to fresh coal after ~60 days to enrich for organisms in the consortium which were actively degrading coal. This initial set of experiments with freshly drilled Big George coal from the Powder River Basin demonstrated the need to acquire coal from a productive basin and to maintain anaerobic conditions as much as possible during sample handling in order to foster growth of the native organisms on the coal itself.

Several recent studies have employed different buffers to control pH in coal microcosm experiments (Harris et al., 2008; Jones et al., 2010), so we sought to examine the effect that different buffers and buffer strengths had on microcosm performance in a systematic manner. Because most active CBM reservoirs are bicarbonate-buffered systems, bicarbonate was a natural choice for our experiments. Organic buffers such as HEPES and PIPES were not considered due to the likelihood of our consortium metabolizing them to form methane. Phosphate is another commonly employed buffer in microbial

incubation experiments, but its use is somewhat limited due to the potential to inhibit acetoclastic methanogenesis at high phosphate concentrations. Figure 12 shows the results of experiments designed to examine the effect of using a phosphate buffer in these microcosm experiments instead of bicarbonate. No significant effect was seen despite previous work showing that phosphate concentrations >20 mM inhibit acetoclastic methanogens (Jones et al., 2010).

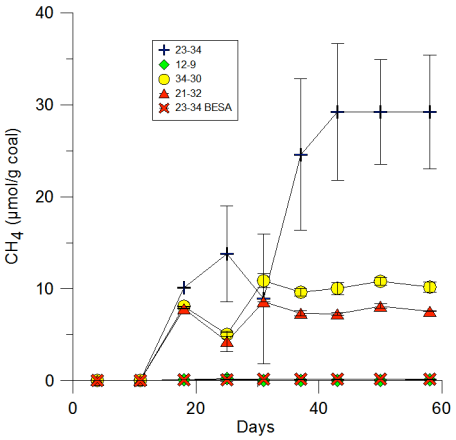

Figure 11. Results of initial incubations showing methane generation by native microorganisms on coal after ~10 days incubation without inoculation (error bars represent 1 σ of triplicate incubations).

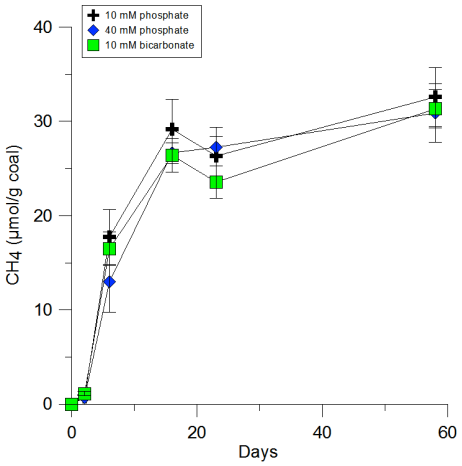

Figure 12. The effects on methanogenesis of buffering microcosm experiments with 10 mM bicarbonate, 10 mM phosphate, and 40 mM phosphate were negligible.

Microcosm experiments were conducted to assess how exposure of coal to oxygen prior to incubation influences the levels of biogas precursor compounds, microbial community structure and methane production. Coal was exposed to air at room temperature to oxidize for 48 hours. Then, the oxidized coal was brought into the anaerobic chamber for 48 hours to remove residual oxygen. The un-oxidized coal was brought into the anaerobic chamber immediately before bottling for incubation. Both coal types, oxidized and un-oxidized, were crushed using a sterile mortar and pestle and bottled, using five grams of

coal, 50 mL of medium and 0.5 mL of inoculum. These microcosms were provided with a 4:1 N_2 to CO_2 headspace and incubated at 30˚C. In the initial experiment, we found that the oxidation of coal lead to decreased methane generation relative to the un-oxidized samples. After seeing this difference, we repeated the experiment and again found that the oxidation of coal resulted in smaller amounts of methane produced when compared to the un-oxidized samples, though the extent of methane production was higher. The results of both experiments are presented in Figure 13.

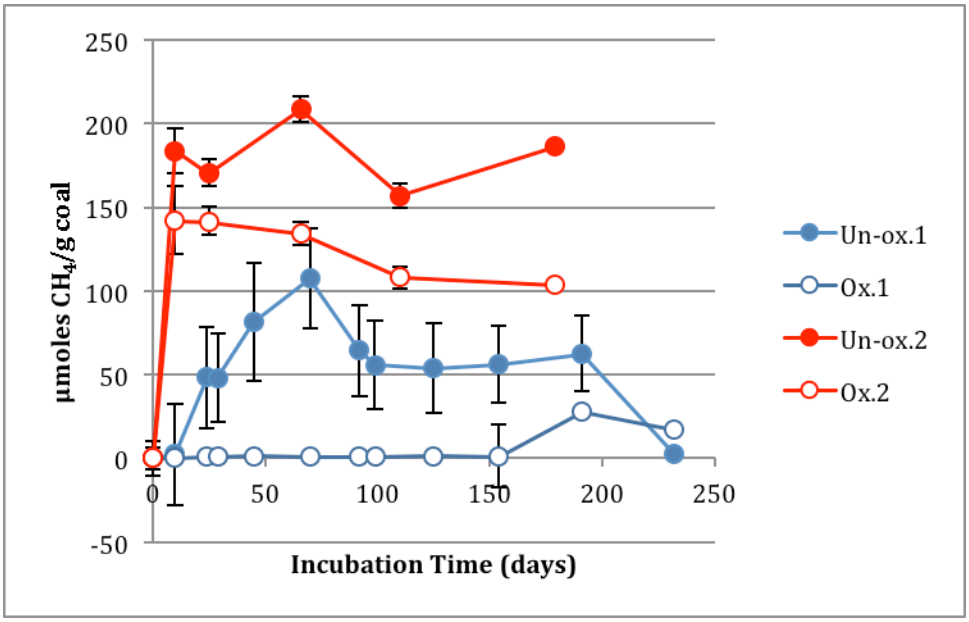

Figure 13. Methane production (cumulative) for first and second oxidized coal experiments. Error bars represent standard error of triplicate bottles.

Acetate was found to be an important precursor in our system. Although the methane production between treatments was clearly different, the results of the levels and types of biogas precursors were not as conclusive. In experiment one, the acetate levels were significantly higher in the oxidized coal samples (and the autoclaved control) than in the un-oxidized samples (Figure 14). This suggests that the oxidation pre-treatment of coal resulted in greater amounts of acetate in the system or the inability of the remaining microbial consortium to utilize acetate. In experiment two, the difference in acetate production between the oxidized and un-oxidized samples was not as significant (Figure 15). Additionally, the amount of acetate measured in the system in experiment two is much lower than what was measured in experiment one. This may be explained in two different ways. One possibility is that the peak in acetate production was not captured for experiment two, which would mean it peaked somewhere between days zero and ten of the incubation and was already mostly consumed by day ten. A second possibility is that the enrichment culture used as an inoculum source in experiment two was better suited to utilize the substrates (e.g., acetate) present, preventing a large build up of acetate before it was converted to methane.

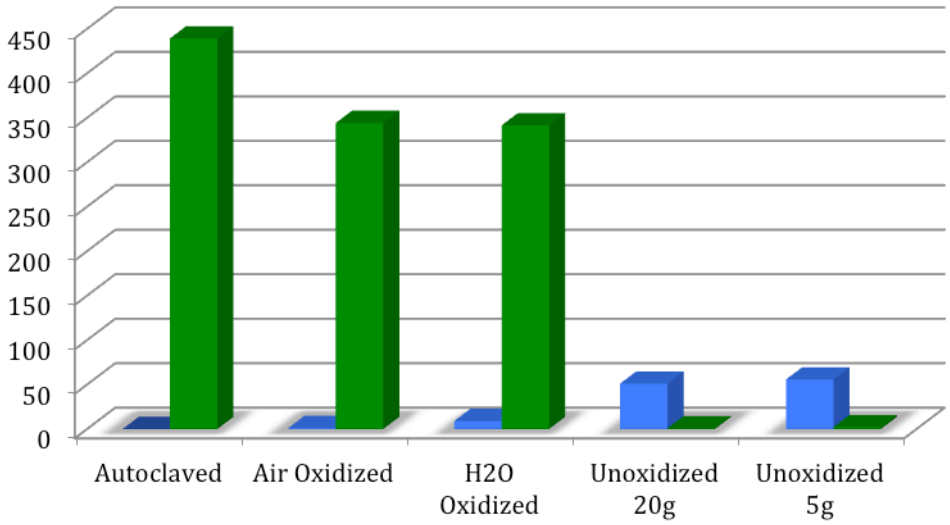

Figure 14. Experiment one acetate values in green (average of three replicates, in mg/L) and methane values in blue (average of three replicates, in micromoles of methane per gram of coal) after 90 days of incubation.

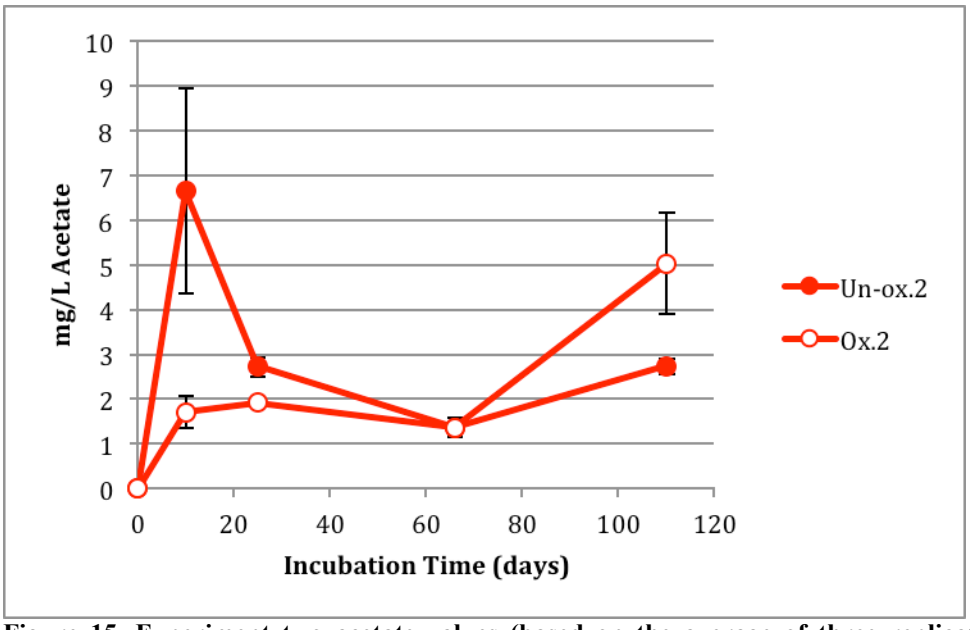

Figure 15. Experiment two acetate values (based on the average of three replicates) over the incubation period. Error bars represent the standard error of the triplicate bottles measured.

7.2: Microbial characterization

Coal is a complex substrate, which supports the idea that a complex microbial community is needed to degrade and utilize the materials available to produce methane. Methanogens play an important role in the system, carrying out the terminal step of coal biodegradation, resulting in methane production. The complexity of this process leaves it largely uncharacterized, which makes identification of the organisms involved in biogas generation from coal significant to the overall understanding of the process. Microorganisms with potential synergistic or antagonistic activities such as fermenters or sulfate reducing bacteria and that had a recurring, significant presence were identified. In addition, characterization of the methanogenic population was employed to determine the relative importance of the two major types of methanogens associated with biogenic methane generation from coal, aceticlastic and CO_2-reducing methanogens.

Following each set of incubation experiments, 1mL samples were collected for DNA extraction, and the remaining sample was frozen and lyophilized before phospholipid fatty acids (PLFA) were extracted. Following the initial cultivation of the consortium from the coal from well 23-34 (Sept. 2009) and subsequent inoculation of new coal degradation experiments, three samples were extracted for phospholipids. The PLFA profile from this set of experiments is depicted in Figure 16. Most PLFAs are ubiquitous across many microbial groups and therefore do not provide taxonomic information, but some are only found in specific genera. For example, the PLFA profile shown in Figure 16 contains the fatty acid iso17:1ω7c which is a biomarker for hydrogen-utilizing sulfate-reducing bacteria (SRB) (Dowling et al., 1988). Additionally, some branched fatty acids, including iso and anteiso 15:0 and 17:0, are generally considered indicative of sulfate reducing bacteria, though not contained exclusively by SRB (Pancost and Sinninghe Damsté, 2003). These PLFAs were commonly found in all coal incubation experiments. Figure 17 shows a PLFA profile for an experiment in which no sulfate was added, though SRB biomarkers were very prominent, including i15:0, ai15:0, 10me16:0, i17:1ω7, i17:0, and ai17:0. The consistency of finding SRB biomarkers in our experiments suggests an important role for SRB within our microbial consortium.

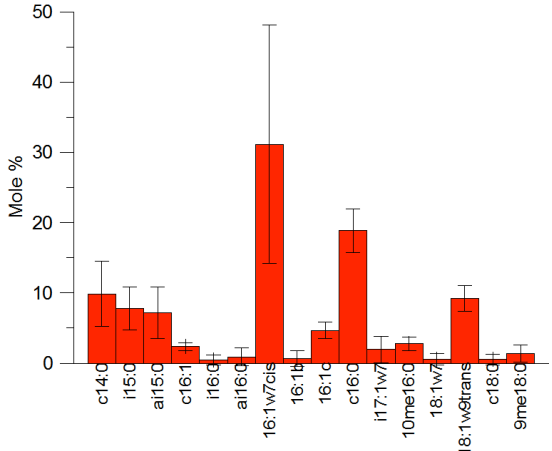

Figure 16. PLFA profile of the microbial consortium enriched from coal after the first set of experiments. Error bars represent 1σ of triplicate extractions.

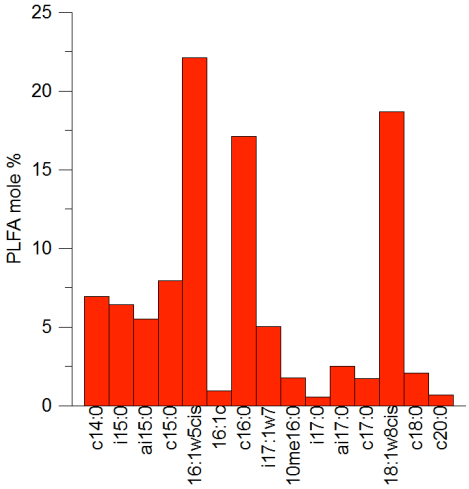

Figure 17. PLFA profile for an incubation experiment without additional sulfate containing SRB biomarkers including i15:0, ai15:0, 10me16:0, i17:1ω7, i17:0, and ai17:0.

In addition to PLFA profiling, genetic analysis of samples was performed, utilizing DNA sequencing technology to characterize the microbial community. Bulk DNA was extracted from raw coal material, the 16S small subunit (ssu) rRNA gene was amplified and sequenced. Figure 18 shows one such sample, from the Werner coal seam in the Powder River Basin, WY. Proteobacteria dominate the microbial community of the sample, including sulfate-reducers, fermenters and other key players in the system (e.g., clostridia, desulfovibrio, etc.). It is interesting that no methanogens were sequenced from the sample, which may indicate bias in the method, low numbers or an actual lack of methanogens. Later incubation experiments with only native coal microorganisms produced methane, suggesting methanogens are present.

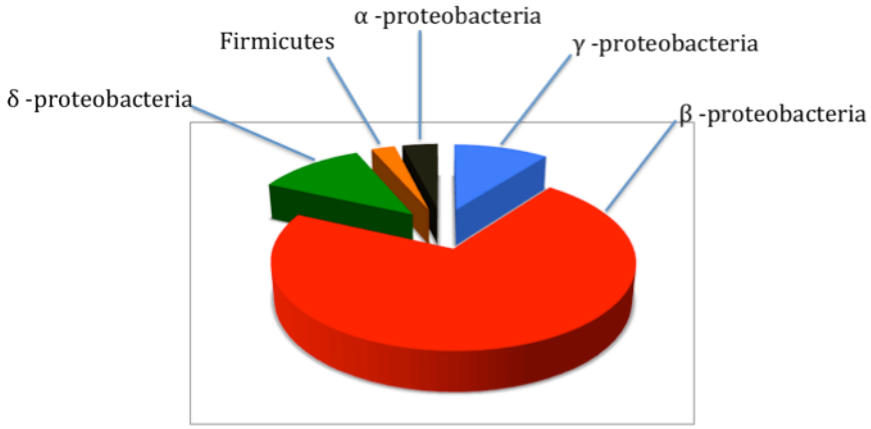

Figure 18. Relative microbial community structure based on Sanger sequencing of the 16S ssu rRNA gene. Sample represents bulk DNA from coal and was not incubated.

Figure 19 shows the microbial community of an enrichment culture used as an inoculum source for several experiments. Similarly to the raw coal, proteobacteria dominate, however, a large portion of the community is methanobacteria. These methanogens are CO_2-reducers. Again we see fermenters such as bacteroidetes, spirochaetes, firmicutes and delta proteobacteria like desulfovibrio. However, no beta proteobacteria were detected, in contrast to the raw coal sample where they made up a large fraction of the population. Over time, we have enriched for a microbial community better suited to biodegrade coal and produce methane. Such incubation led to an alteration in the community structure, possibly selecting for organisms that outcompete others or have more diverse metabolic capabilities.

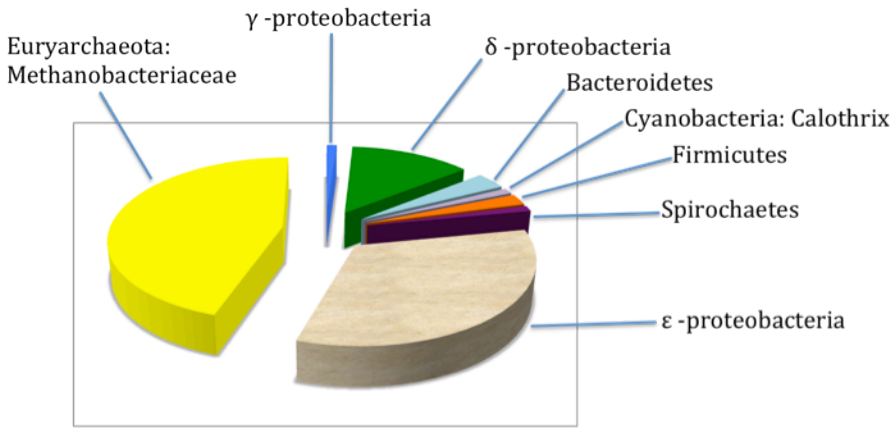

Figure 19. Relative microbial community structure based on Sanger sequencing of the 16S ssu rRNA gene. Sample represents bulk DNA from enrichment culture used as inoculum for several experiments.

With regard to the methanogenic population, the makeup of this population appears to change over time. Additionally, experimental variability could account for some of the apparent shift in the methanogenic population. Figure 20 shows the changes in three samples' methanogen populations over time and within sample treatment replicates. Sample one represents the community present in the

inoculum source used for this experiment. Methanobacteria were the dominant methanogen type found in this sample. These organisms reduce carbon dioxide to produce methane. Interestingly, sample two is an incubation from this experiment that produced significant amounts of methane (97 µmol CH_4/g coal). In this sample, the methanogen population is made up of Methanosarcina, which are aceticlastic methanogens known to have versatile metabolic capabilities. This is an example of how the methanogen population changed over time. Incubation may have selected for methanogenic organisms with more versatile metabolic capabilities, since it was a closed system where no new substrate was added over time. Additionally, there was variability between replicates. Samples two and three (Figure 20) were set up with the same contents under the same conditions but resulted in different microbial community structure. Sample two had a significant methanogen population, while sample three did not. This was also evident in the methane production. Sample two, with the large methanogen population, produced appreciable amounts of methane. However, sample three, with the very small methanogen population, did not (3.5 µmol CH_4/g coal).

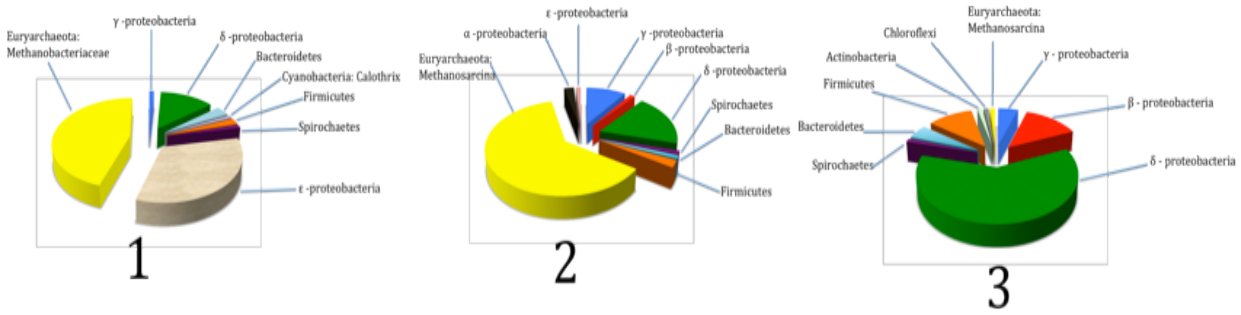

Figure 20. Relative microbial community structure based on Sanger sequencing of the 16S ssu rRNA gene. Sample 1 is the inoculum source, sample 2 is an incubated sample with high methane production, and sample 3 is an incubated sample with low methane production.

In addition, the microbial communities in the oxidized coal experiments were characterized with DNA pyrosequencing techniques. Figure 21 demonstrates the effect that coal oxidation has on the microbial community. Oxidation, in this case, appears to result in a less diverse community as compared to the un-oxidized sample.

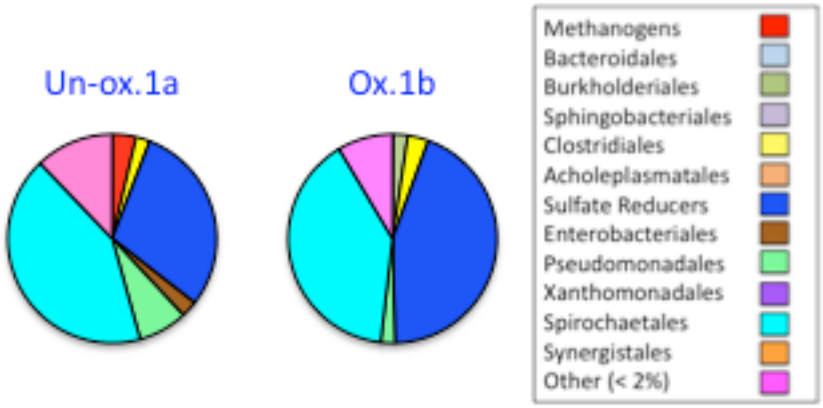

Figure 21. Microbial community structure based on 454 pyrosequencing of the 16S ssu rRNA gene.

In addition to coal oxidation, other incubation amendments were examined. Although the amount of methane production was not significantly affected based on the amendment, differences in the microbial community structure were apparent. Figure 22 shows three samples with different amendments. The "un-inoculated" sample has coal (including native organisms), medium and no inoculum. The "sulfate medium" sample has coal, medium (with sulfate 5mM) and inoculum. The "sodium sulfide" sample has coal, medium, inoculum and 80 µM sodium sulfide, which acts as a chemical reductant. Interestingly, the un-inoculated sample has the largest population of methanogens of the three samples. The sulfate-reducer population is larger in the sulfate medium than the other samples, which is expected because sulfate is their preferred substrate. The clostridia population is larger in the sodium sulfide sample, which may be explained because clostridia are strict anaerobes, so the addition of a chemical reductant may have helped to keep this microcosm at an anoxic level that best suits these organisms.

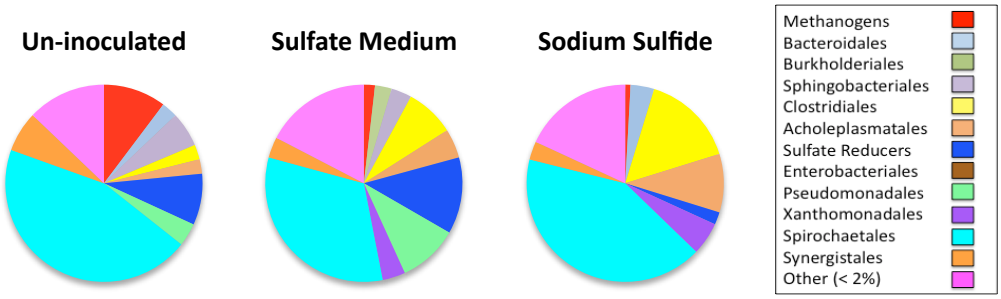

Figure 22. Relative microbial community structure based on 454 pyrosequencing of the 16S ssu rRNA gene. Labels indicate incubation condition differences between samples.

7.3: Identification of metabolic intermediates and capabilities of the microbial community.

A experiment was conducted to identify whether preparing coal under different gas conditions caused different methane production. Hydrogen, carbon dioxide, or both were injected into serum bottles with ground and rinsed Big George coal. The headspace gas was analyzed after Big George coal was exposed at different gas conditions for 12-12.5 hours. The results are summarized in Table 6. Hydrogen decreased

in all cases when it was added. The decrease could be due to consumption by organisms or adsorption onto coal. The amount of carbon dioxide increased when no additional carbon dioxide was added. This suggests that adsorbed carbon dioxide was released from coal to maintain equilibrium between gas and solid phase. However, the amount of carbon dioxide decreased when additional carbon dioxide was added suggesting that carbon dioxide was either adsorbed by coal to maintain equilibrium between gas and solid phase or was consumed by organisms or some combination. The amount of methane increased for each condition but the differences between the conditions were not significant, suggesting that methane was desorbing from coal, as opposed to being actively produced microbially.

Table 6. Amount of Gas for Big George Coal Exposed under Different Gas Conditions for 12-12.5 Hours

Conditions	Time zero , µmol/bottle			Δ[a], µmol/bottle		
	H_2	CO_2	CH_4	H_2	CO_2	CH_4
N_2, n[b]=2	0	4.7±6.6	0	0	(+)[c]11.2±5.8	(+)2.7±0.6
N_2+CO_2 (A)[d], n=2	0	524.0±37.8	0	0	(–)[e]109.1±54.7	(+)2.7±2.3
N_2+H_2 (A), n=2	345.5±22.7	9.6±1.5	0	(–)28.4±37.5	(+)6.9±0.4	(+)6.2±0.8
N_2+CO_2 (B)[f]+H_2 (B), n=5	165.2±3.8	270.0±9.2	0	(–)25.9±22.6	(–)64.02±28.1	(+)2.8±2.1
N_2+CO_2 (A)+H_2 (B), n=5	334.2±10.7	505.3±40.7	0	(–)20.9±24.8	(–)87.0±30.9	(+)5.1±0.9

[a] Δ=Amount of gas after 12-12.5 hours-Amount of gas at time zero
[b] n=replication
[c] (+) = gas amount increased
[d] A=10 mL gas
[e] (–) = gas amount decreased
[f] B=5 mL gas

Each experimental bottle then received 50 mL of basal medium and the headspace was purged with nitrogen (UHP). 0.5 mL of sub-culture 23-34 γ inoculum in UW medium was injected into each experimental bottle with UW medium. Methane production from these systems is shown in Figure 23. Methane was produced from each coal culture after coal was exposed at gas conditions for 12-12.5 hour. Additional inoculum did not enhance methane production and instead the highest methane production occurred in bottles that did not receive inoculum other than the coal itself. Methane production from coal exposed to both hydrogen and CO_2 prior to adding medium was higher than from coal exposed to other gas conditions.

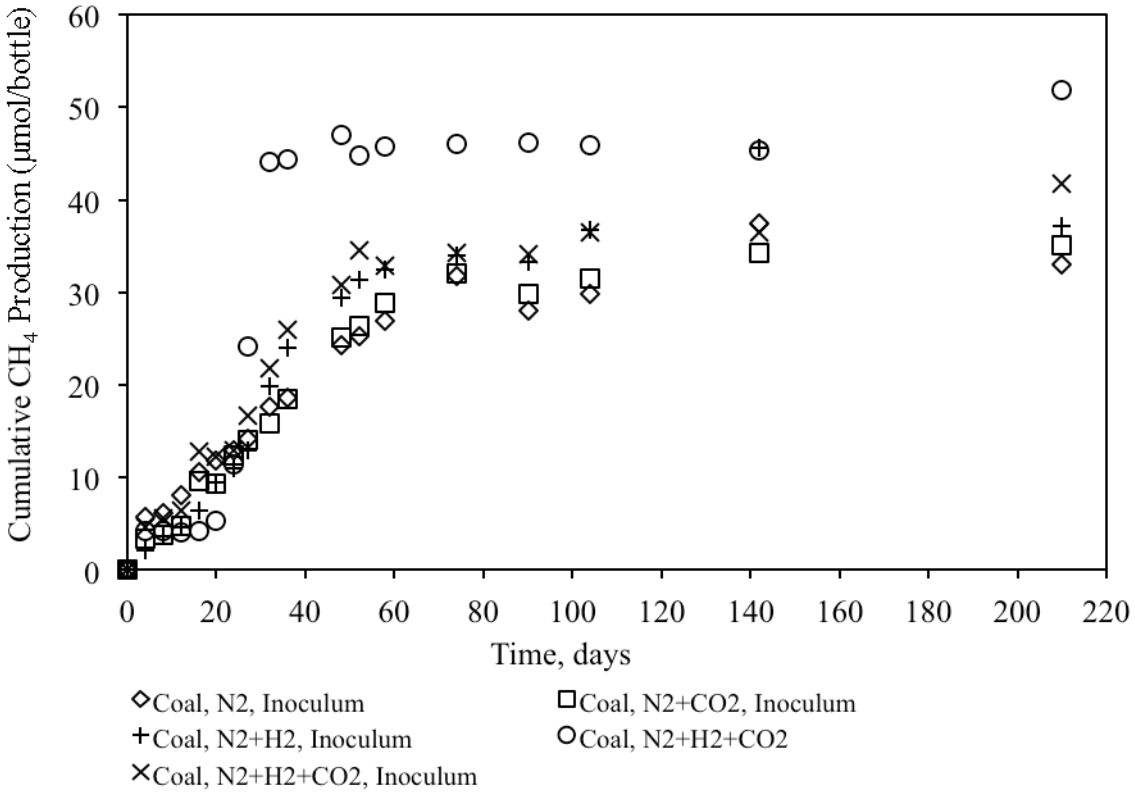

Figure 23. Biogenic Methane Production after Coal Exposed at Different Gas Conditions for 12-12.5 Hours.

Five conditions were examined to identify the potential for methane production from coal cultures (

Table 7). The only condition to produce methane was the L-cysteine condition. The Sulfate condition included the same constituents as the L-cysteine condition but also contained sufficient sulfate to consume 130 mg COD/L. The absence of methane production suggests that sulfate reducing activity consumed electrons that would have otherwise been available for methane production. The absence of hydrogen production in the Sulfate condition further suggests that sulfate-reducing activity was possible directly with available substrate without the need for fermentation.

Table 7. Hydrogen and Methane Production from Different Treatments[1]

	Condition	Sulfate (mg/L)	L-cysteine (mg/L)	Vitamin	Autoclaved	H_2 Production (Max.± Std. Dev.) (µmol/bottle)	CH_4 Production (Max.± Std. Dev.) (µmol/bottle)
1	Sulfate	195	300	Added[2]	No	N.D.[3]	N.D.
2	L-cysteine	0	300	Added	No	50.3±24.4	7.8±3.4
3	Autoclaved	0	300	Added	Yes	N.D.	N.D.
4	Vitamin	0	0	Added	No	N.D.	N.D.
5	Coal Only	0	0	Not added	No	N.D.	N.D.

[1] All treatments received coal as the only inoculum source.
[2] Vitamin solution as indicated in methods.
[3] Not detected.

The Autoclaved condition was set up identically to the L-cysteine condition but was autoclaved after coal addition. The absence of hydrogen and methane production in the Autoclaved condition suggests that the added coal was the source of the microbial community that facilitated fermentation and methanogenesis in the L-cysteine condition.

The Vitamin condition differed from the L-cysteine condition by not having L-cysteine added while the Coal Only condition had neither L-cysteine nor vitamins added. Both conditions received coal as the inoculum source but neither condition produced hydrogen or methane. This apparent lack of fermentative and methanogenic activity is not likely due to competition from sulfate-reducing activity because neither condition received sulfate. These results suggest that hydrogen and methane production in the L-cysteine condition were due to the consumption of added L-cysteine by a microbial community present in the coal but not able to readily degrade the coal matrix itself.

The pattern of methane production from L-cysteine suggests that L-cysteine was first fermented to produce hydrogen followed by hydrogenotrophic methanogenesis (Figure 24). Hydrogen was first detected by day 3 and then stayed approximately constant until methane production initiated five days later. Unlike hydrogen production, which initiated and was effectively completed within one day (between days 2 and 3), methane production and concurrent hydrogen consumption occurred slowly after initiation with hydrogen no longer detected and methane production maximized 9 days after initiation.

To further evaluate the hydrogenotrophic methanogenesis that occurred in the L-cysteine-fed bottles, additional hydrogen was added on day 35 (Figure 25). Hydrogen consumption and methane production occurred concurrently, stoichiometrically and more rapidly than previously in the same bottles. The population of hydrogenotrophic methanogenic organisms that was originally present in the coal at inoculation appeared to have grown slowly upon initial exposure to hydrogen but growth was sufficient to facilitate rapid methanogenesis when re-exposed to hydrogen.

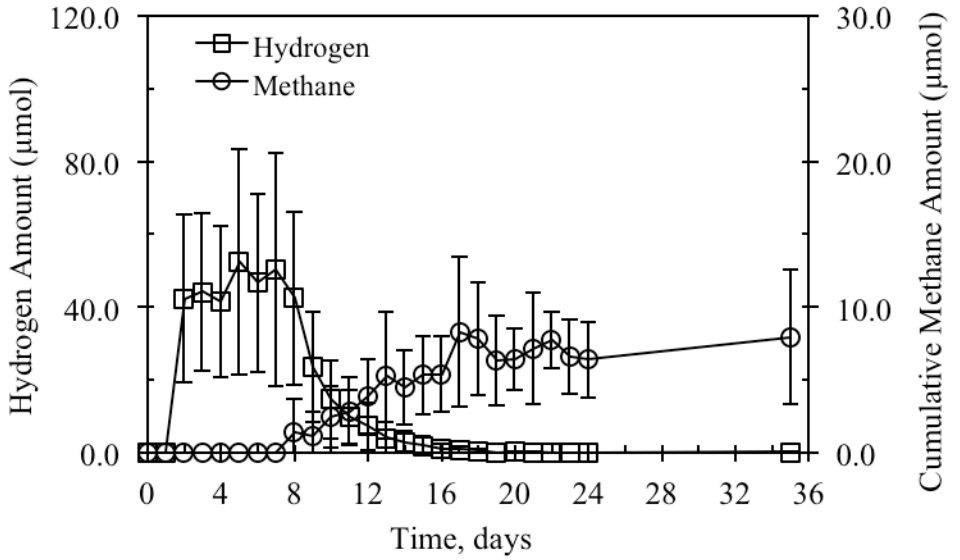

Figure 24. Hydrogen and cumulative methane production by coal cultures with L-cysteine. Error bars represent standard deviation for triplicate cultures.

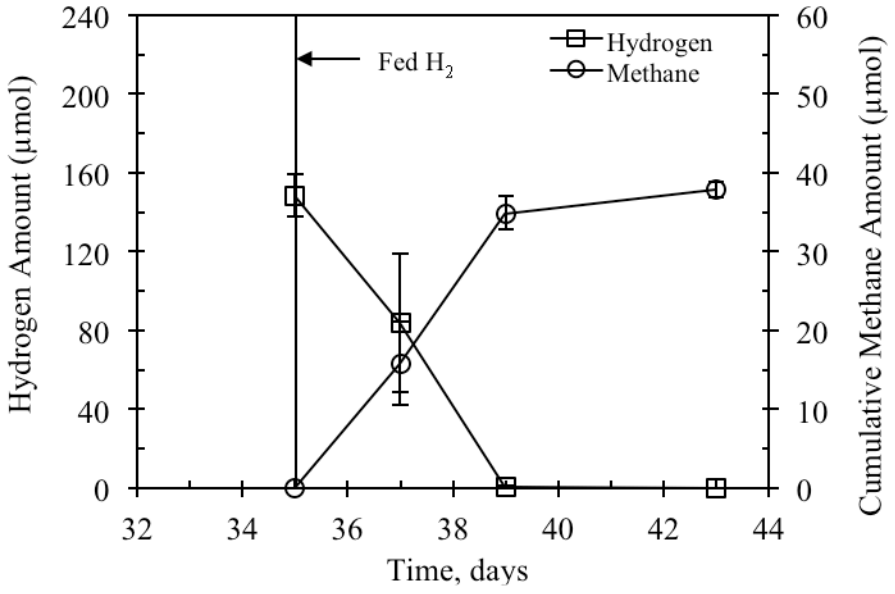

Figure 25. Hydrogen and cumulative methane production by coal cultures with L-cysteine after receiving H_2 one time. Error bars represent standard deviation for triplicate cultures.

The presence of aceticlastic methanogens was not detected. A set of bottles prepared with coal as the only inoculum and receiving acetic acid (60 mg/L) produced no methane over 100 days of incubation. Aceticlastic methanogens were either not present in the coal or were inhibited in some manner.

To investigate whether ethanol can stimulate or enhance methane production from coal, three different amounts (1, 5 and 10 mg) of filter sterilized ethanol were injected into the experimental bottles with 10 g of ground and sterilized water-rinsed Big George coal. Methane was produced from experimental bottles with coal and added ethanol during 36 days of incubation (Figure 26).

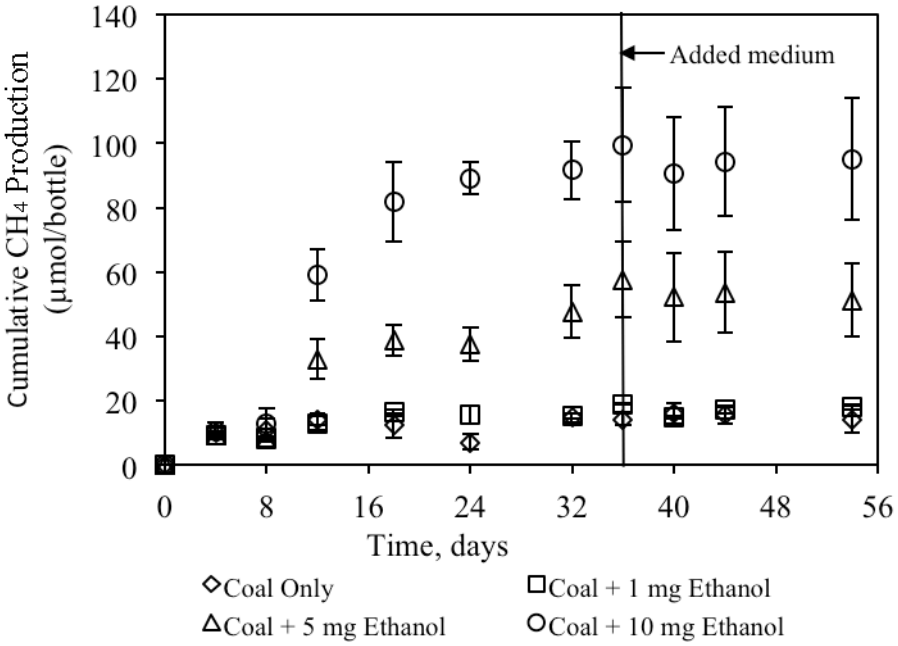

Figure 26. Cumulative methane production from coal receiving different amounts of ethanol. Error bars represent standard deviation for triplicate cultures.

On day 36, 2.5 mL sterilized water was added into each bottle, and 0.5 mL liquid was withdrawn to measure the pH. Then, 3 mL MUW medium was added. However, no new methane was produced during the following 18 days of incubation (Figure 26). The measured pH values and calculated COD values are summarized in Table 8. The ethanol was degraded by fermentative organisms to produce acetic acid or hydrogen, and then methanogens used the produced substrate to produce methane. However, acetic acid detected from the liquid sample suggests that aceticlastic methanogens were either not present in the examined coal sample or were inhibited, although the pH values indicate that pH was not the inhibition factor. Over 60% of the added COD was not detected in the products measured. This might have been converted to unidentified compounds (e.g. lactic acid, pyruvate), adsorbed by the coal, or used for biomass growth. Regardless, organisms (fermenters and hydrogenotrophic methanogens) on the coal itself were able to degrade added ethanol to produce methane even when the coal was not supplied with medium and inoculum.

Table 8. Measured pH and Calculated COD in Coal Receive Different Amount of Ethanol

Conditions	pH		COD, mg/bottle			COD recovery[c], %
	pH[a]	pH[b]	Iso-propanol	Acetic acid	Max. CH_4	
Coal	7.3±0.1	7.3±0.1	0	0	1.1±0.1	—
Coal + 1 mg Ethanol[d]	7.2±0.1	7.3±0.1	0.04±0.01	0	1.2±0	7.0±0
Coal + 5 mg Ethanol[e]	7.0±0.1	7.1±0.1	0.2±0.01	0.9±0.4	3.7±0.8	34.3±7.6
Coal + 10 mg Ethanol[f]	6.7±0	6.9±0.1	0.2±0.1	2.1±0.2	6.8±0.6	38.3±2.9

[a] pH was measured after water was added to each bottle.
[b] pH was measured on Day 54 (the last day of incubation).
[c] COD recovery, % =(Sum of the identified COD – $COD_{\text{background methane from coal}}$)×100%/ Received COD, Sum of the identified COD = $COD_{\text{Iso-propanol}}$+$COD_{\text{acetic acid}}$+$COD_{\text{methane}}$,
$COD_{\text{background methane from coal}}$=1.1 mg COD/bottle
[d] 1 mg ethanol=2.1 mg COD
[e] 5 mg ethanol=10.5 mg COD
[f] 10 mg ethanol=21 mg COD

To examine whether medium and added inoculum would enhance methane production from coal, three different amounts (1, 5 and 10 mg) of filter sterilized ethanol were injected into experimental bottles with 10 g of ground and sterilized water rinsed Big George coal. After 1 hour, 5 mL MUW medium was injected to each experimental bottle to avoid losing produced hydrogen or evaporated ethanol. 0.5 mL of 23-34 γ inoculum (in Tanner medium) was used in this experiment. Methane was produced from each coal cultures containing ethanol, medium and inoculum during 54 days of incubation (Figure 27). Methane production from coal cultures with ethanol was lower than the theoretical methane production expected from ethanol. After coal cultures with ethanol were incubated 62 days, the headspace of culture bottles was purged with N_2 to remove accumulated methane and hydrogen. With further incubation, additional hydrogen and methane was detected from coal cultures that were initially supplied with 5 and 10 mg ethanol (Figure 28).

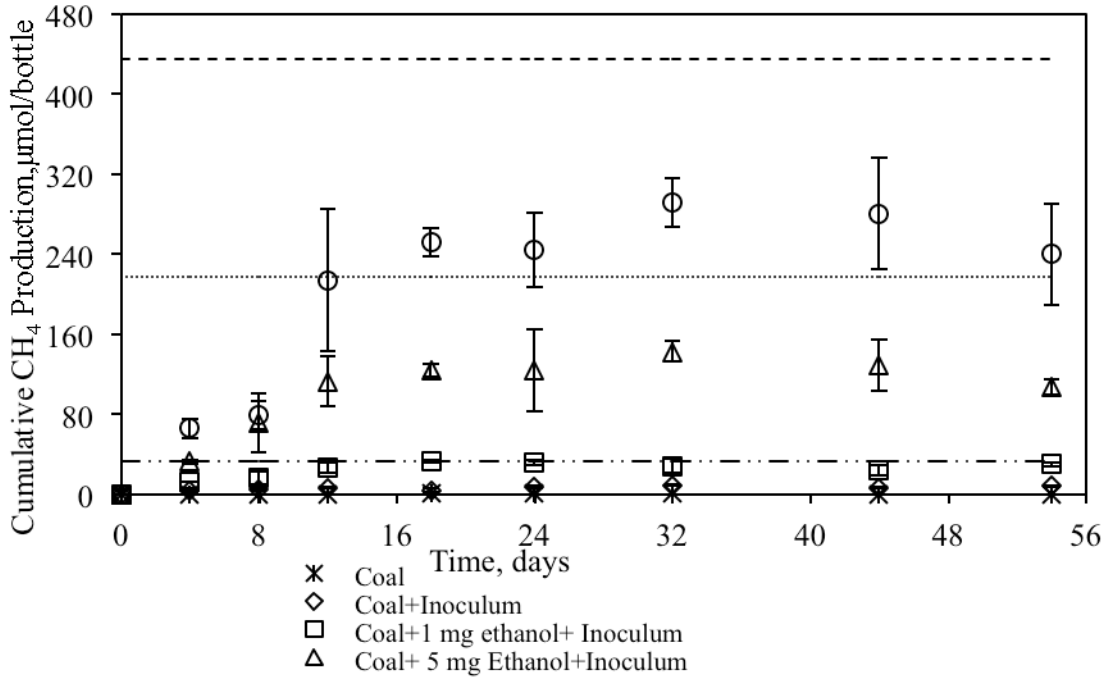

Figure 27. Cumulative methane production by coal cultures receiving medium, ethanol or inoculum. Error bars represent standard deviation for triplicate cultures.

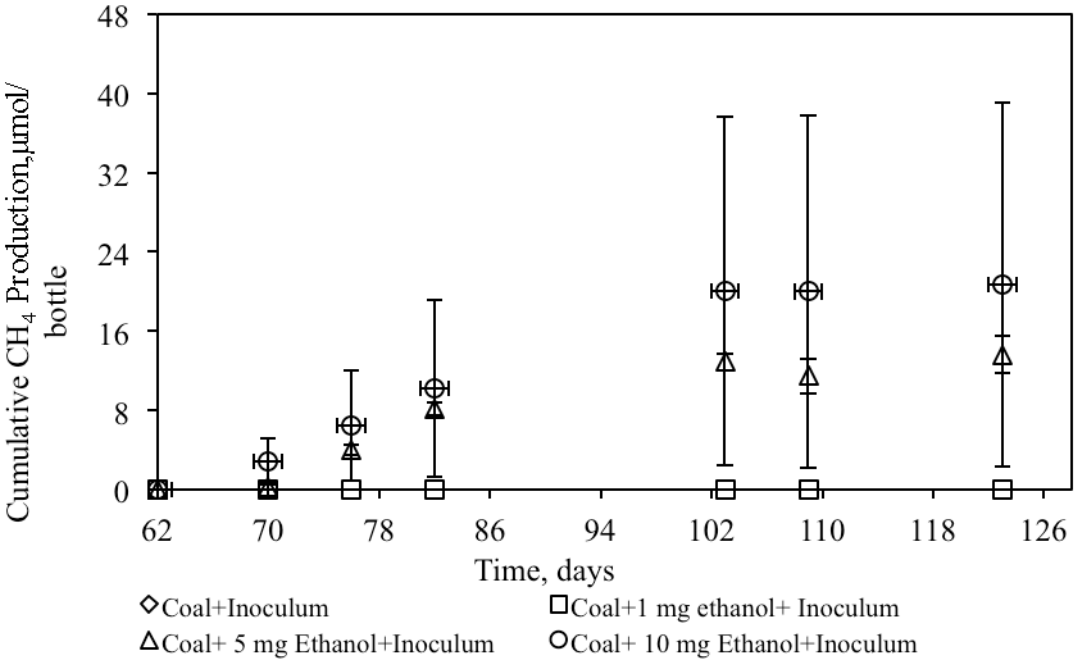

Figure 28. Cumulative methane production by coal cultures receiving medium, ethanol or inoculum (days 62-126 of incubation). Error bars represent standard deviation for triplicate cultures.

The measured pH and calculated COD are summarized in Table 9. The ethanol recovery ratio from coal cultures supplied with 5 and 10 mg ethanol was 96.1±0.4% and 98.1±4.7%, respectively, higher than

the 74.5±2.4% COD recovery ratio in the coal culture with 1 mg ethanol. The COD recovery ratio in ethanol control cultures (ethanol, inoculum, medium, and without coal) was 53±9.9%, 61±2.1%, and 51±26.9% for 1, 5, and 10 mg ethanol, respectively. The conversion of ethanol to acetic acid and other possible organic acids (such as lactic acid, which was not measured) decreased the pH of ethanol control cultures to 5.5-6. The activity of methanogens and fermenters were likely inhibited at these low pH values.

Table 9. Measured pH and Calculated COD in Coal Receiving Medium, Inoculum, and Different Amounts of Ethanol

Conditions	pH	COD, mg/bottle		COD recovery[a], %
		Iso-propanol	Max. CH_4	
Coal+Medium +Inoculum	7.3±0.04	0	0.6±0.02	
Coal +Medium+Inoculum+1 mg Ethanol[b]	7.2±0.01	0	2.14±0.05	74.5±2.4
Coal +Medium Inoculum+ 5 mg Ethanol[c]	7.2±0.03	0.1±0	10.6±0.04	96.1±0.4
Coal +Medium Inoculum+10 mg Ethanol[d]	7.3±0.03	0.1±0.08	21.1±1.1	98.1±4.7

[a] COD recovery, %
=(Sum of the identified COD – $COD_{\text{background methane from coal}}$)×100%/ Received COD,
Sum of the identified COD = $COD_{\text{Iso-propanol}}$+$COD_{\text{methane}}$,
$COD_{\text{background methane from coal}}$=0.6 mg COD/bottle

In order to better understand the chemical functionalities of the coal that are degraded by the consortium, experiments with several different model compounds were conducted. The compounds chosen included a range of functionalities, including straight chain aliphatics (hexadecane), substituted aromatics, and long chain fatty acids. The results for the hexadecane experiments are shown in Figure 29. Hexadecane was not shown to be degradable by the consortium of organisms enriched from coal in our study, which is consistent with the recent findings of Jones et al. (2010). In addition several monosubstituted aromatic hydrocarbons were tested with the microbial consortium enriched from PRB coal in order to determine if the degradable portion of the coal was aromatic in functionality. The compounds tested included toluene, benzoate, and *m*-xylene. None of these compounds enhanced methanogenesis over the unamended control (Figure 30), indicating that they were not viable carbon sources on their own. Toluene and *m*-xylene actually showed an inhibitory effect on our consortium at the concentration tested, though this may not be true at lower concentrations.

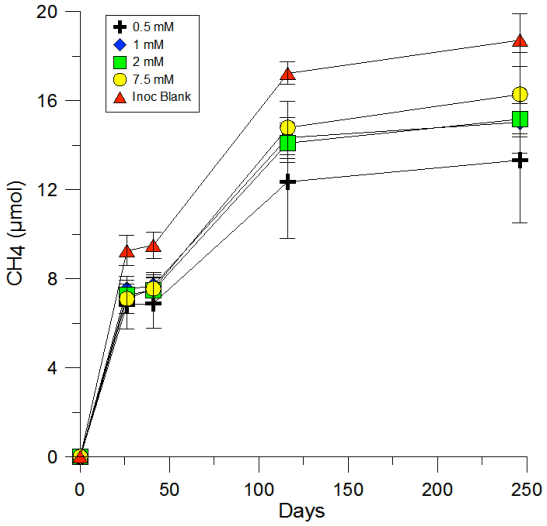

Figure 29. The microbial consortium enriched from coal in this study was unable to degrade hexadecane.

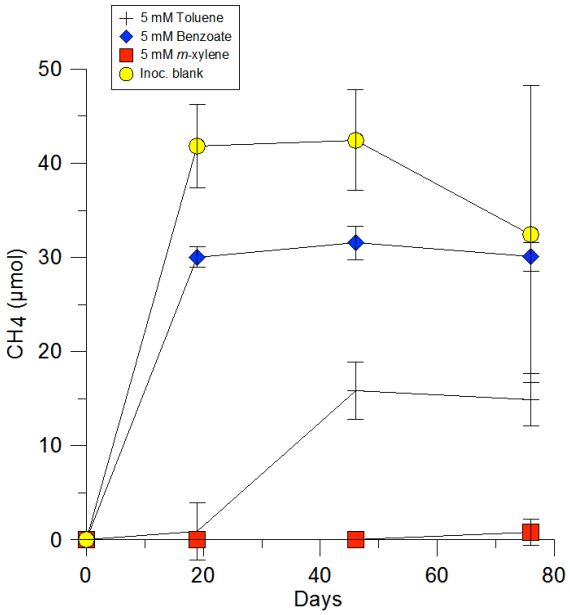

Figure 30. The microbial consortium enriched from coal was not able to utilize any of the mono-substituted aromatics tested at the concentrations shown above.

In every experiment that produced methane, acetate was found to be a key intermediate in the process. Figure 31 shows a typical methane and acetate profile for experiments with only coal as a carbon substrate. Acetate is produced rapidly from fermentative organisms and then depleted almost entirely by week 3 of the incubation. In experiments amended with 33 mg/L 4-nitrophenol to inhibit acetoclastic methanogenesis (Bhattacharya et al., 1995), acetate was not consumed and very little methane was produced. The effect of inhibiting acetoclastic methanogens with 4-nitrophenol is depicted in Figure 32. This effect could only be studied for ~3 weeks as 4-nitrophenol was degraded by our consortium in longer experiments.

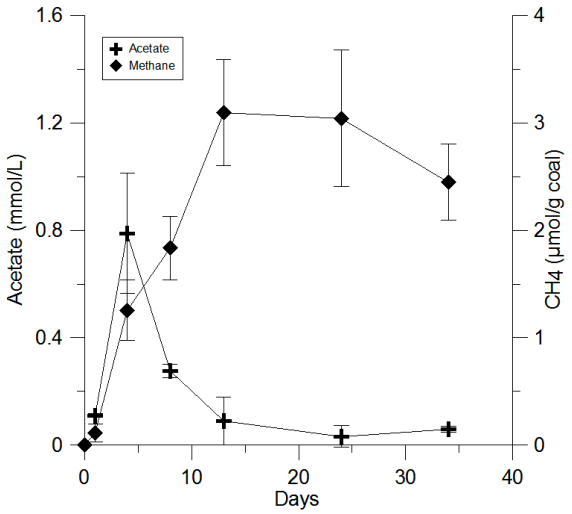

Figure 31. Acetate and methane profiles for a typical experiment.

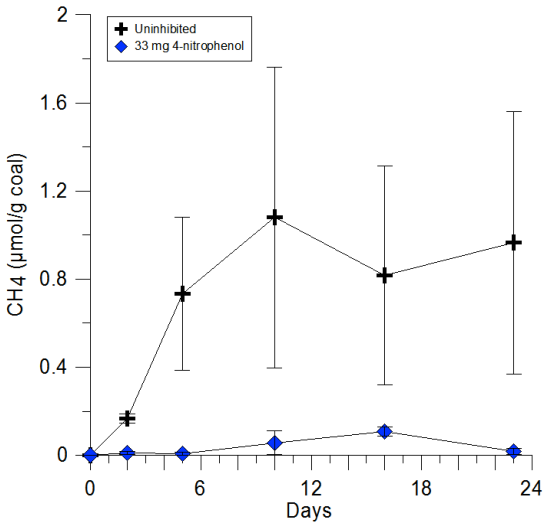

Figure 32. Inhibiting acetoclastic methanogens with 4-nitrophenol causes a dramatic reduction in methane production from coal.

We also examined the role of SRB in methanogenic coal degradation experiments through the use of variable sulfate concentrations (50 µM – 1mM) and metabolic inhibitors (5 mM molybdate for SRB). Molybdate functions as a metabolic inhibitor for SRB due to its passive uptake into the cells of SRB wherein it interferes with the formation of reduced sulfur compounds needed for growth (Patidar and Tare, 2005). We hypothesized that with increasing sulfate concentrations SRB would outcompete methanogens for both the acetate and hydrogen resulting from coal fermentation, and that the absence of sulfate, or presence of molybdate, would enhance methanogenesis relative to the uninhibited, sulfate-amended experiments. Results from these experiments suggest that SRB did not outcompete methanogens for available acetate or hydrogen because methane production did not depend on sulfate concentration

(Figure 33). Roughly 4-6 µmol sulfate was consumed in each experiment amended with sulfate, regardless of its starting concentration (Figure 34). Experiments performed with molybdate and in the absence of sulfate did not produce more methane than experiments amended with up to 1mM sulfate, suggesting that SRB did not compete with methanogens for the same substrate. This is also consistent with our finding SRB biomarkers in experiments not amended with sulfate.

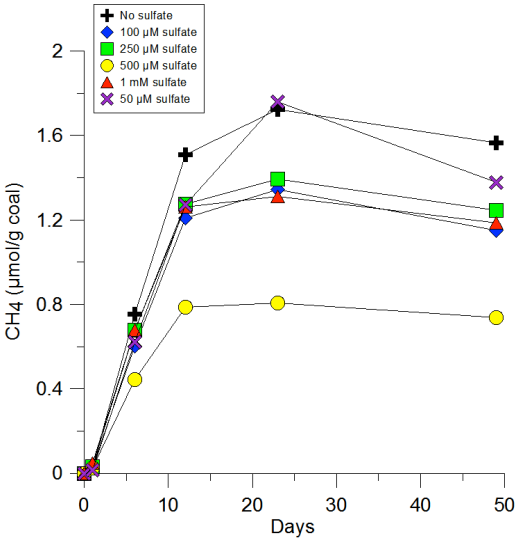

Figure 33. Sulfate amendment did not significantly affect methane production in coal microcosms despite active SRB.

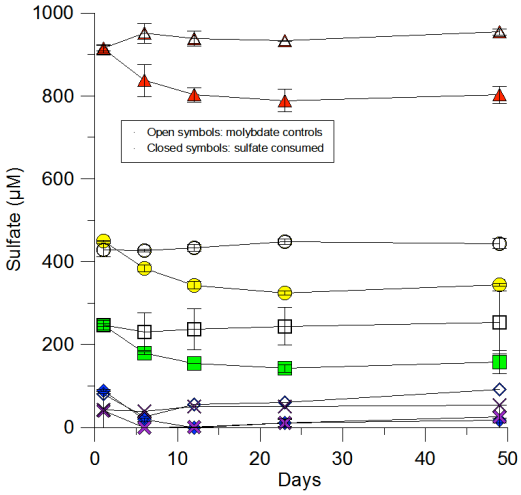

Figure 34. Sulfate consumption in the uninhibited experiments (solid symbols) was independent of the starting sulfate concentration.

Task 8.0—Modeling

Objective: Capture chemical and microbial dynamics of coal conversion to methane in a computer model, to allow comparisons of different incubation scenarios (project objective 6).

The hydrogen consumption and biomass growth rates for the Smith coal cultures were simulated using a Monod-type model. The yield (Y) was assumed to be 0.008 μmol VSS/μmol substrate consumed (Rittmann and McCarty, 2001) while X_0 was assumed to be 0.4 μmol VSS/bottle. The measured S_0 was 156.8 μmol/bottle. The estimated values of K_s and k from weighted, nonlinear least-squares regression analysis were 28.4 μmol/bottle and 13.6 μmol substrate /μmol biomass·day, respectively. The k and K_S estimates represent the overall average values for the different hydrogen-consuming organisms in the coal culture. When batch reactors were first exposed to H_2, the assumed values of Y and X_0, estimated values of K_S and k, and measured values of S_0 were used to obtain the simulated hydrogen consumption curve (

Figure 35). The actual hydrogen consumption rate was slower than the simulation results for the first exposure but after the second exposure to hydrogen, the hydrogen consumption rate was simulated well by the model (

Figure 35).

To further evaluate the model, it was used to simulate data from the Coal Only condition (coal culture with neither L-cysteine nor vitamin solution), using the parameter values of k, K_S, Y and X_0 determined from the Vitamin condition (coal culture with vitamin solution but without L-cysteine). The model curves fit the experimental data well for both H_2 exposures (Figure 37).

The Monod-type model ignored changes in biomass due to decay. Nevertheless, the predicted biomass was not constant, and increased with the hydrogen consumption. The simulation curves of biomass growth in the Coal Only condition and Coal Only condition are shown in Figure 36 and Figure 38, respectively. The predicted biomass growth rate was slower with the first exposure to H_2 than with the second exposure to H_2. Presumably, the increased H_2 consumption rates (

Figure 35 and Figure 37) were due to growth of the microbial community.

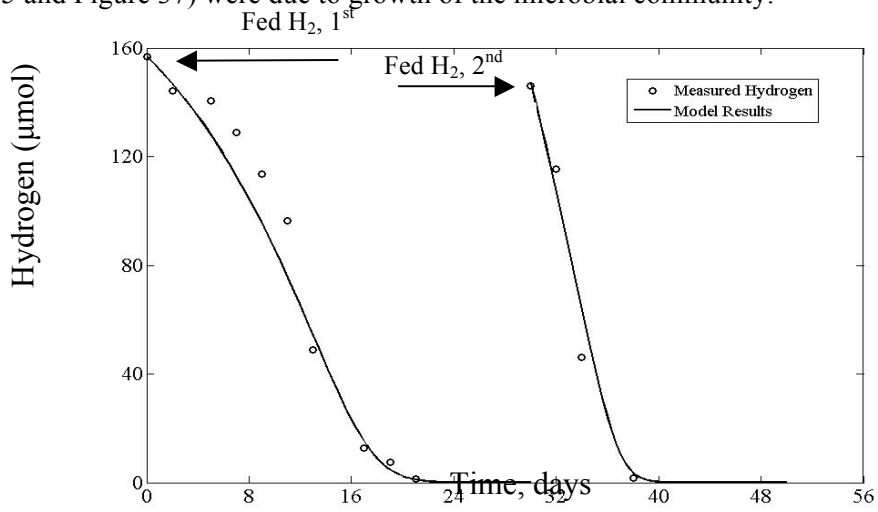

Figure 35. Comparison between the model simulations and the experimental data in coal culture with vitamin solution without L-cysteine.

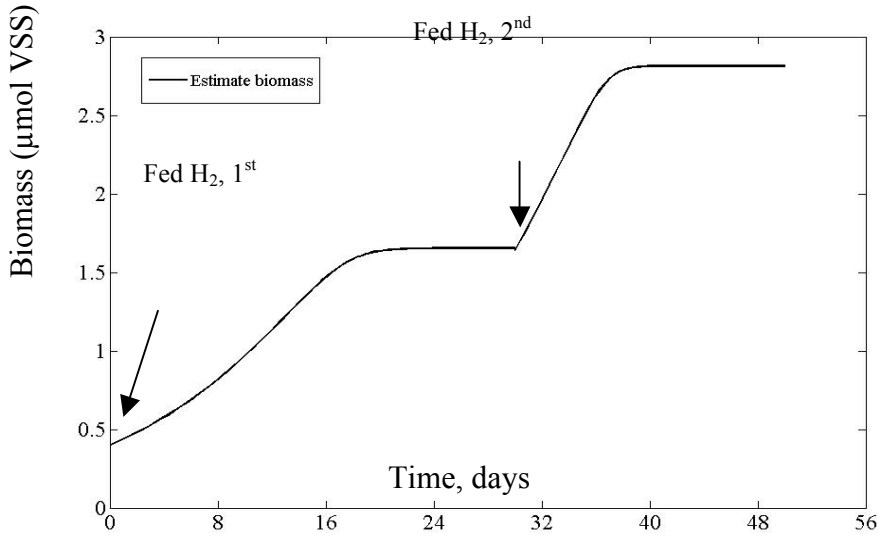

Figure 36. Estimated biomass growth in coal culture with vitamin solution without L-cysteine.

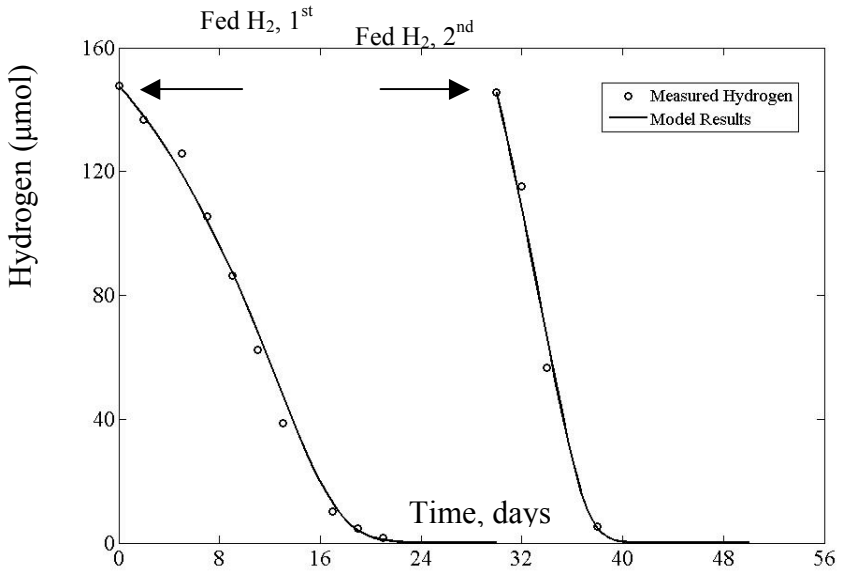

Figure 37. Comparison between the model simulations and the experimental data in coal culture with neither L-cysteine nor vitamin solution.

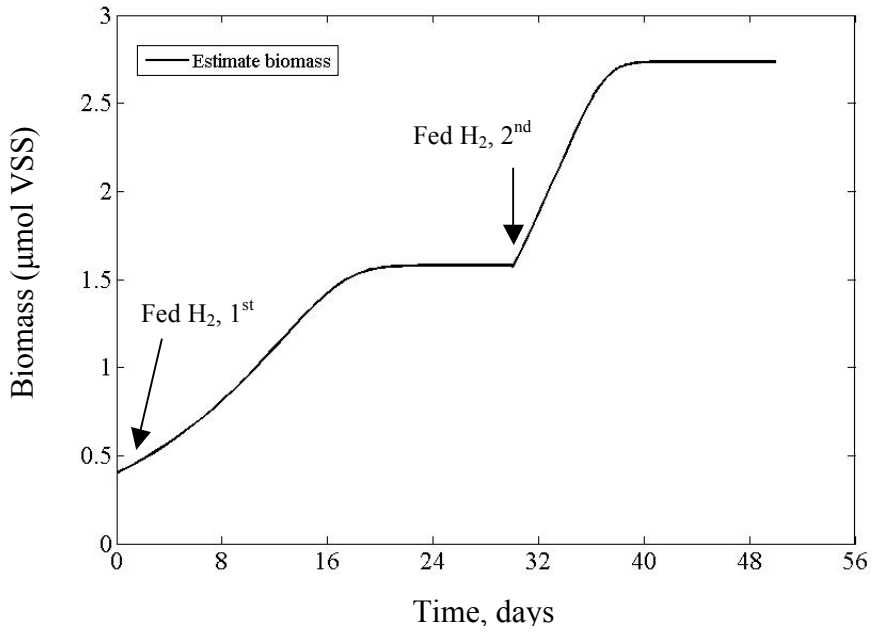

Figure 38. Estimated biomass growth in coal culture with neither L-cysteine nor vitamin solution.

The modeling effort will continue beyond the project period, so that dynamics of the microbial community and other intermediate substrates can be captured.

Publications and Presentations:

Enhanced microbiological generation of coalbed methane. Presentation by L. K. Gallagher, J. Munakata-Marr, L. Landkamer, L. A. Figueroa, A. W. Glossner, K. Mandernack, S. H. Harris, Y. Liu, D. Bagley, W. Rodgers, F. Basile, Z. Huang, M. Urynowicz, 2009. National Meeting of the American Society of Mining and Reclamation, Billings, MT. R.I. Barnhisel (Ed.) Published by ASMR.

Coal Pre-Treatment and Its Effects On Extractable Organic Matter. Presentation by L. K. Gallagher, S. H. Harris and J. Munakata-Marr, 2010. Energy Resources and Produced Water Conference, Laramie, WY.

Enhanced microbiological generation of methane from coal. Presentation by L. K. Gallagher, A. W. Glossner, L. Landkamer, K. Mandernack and J. Munakata-Marr, 2010. International Symposium on Microbial Ecology, Seattle, WA.

Microbial methanogenesis from a consortium enriched from the Powder River Basin, WY. Presentation by A. W. Glossner, L. K. Gallagher, L. Landkamer, L. A. Figueroa, J. Munakata-Marr and K. W. Mandernack, 2010. Goldschmidt Conference, Knoxville TN.

Pressurized heating for the rapid preparation/extraction of coal samples for GC-MS analysis.
F. Basile W. Rodgers and R. K. Mahat. Manuscript in preparation, to be submitted to: Energy and Fuels

Secondary Biogenic Coal Bed Natural Gas in the Powder River Basin. Invited talk by M.A. Urynowicz and Z. Huang, 2011. New Horizons in Oil and Gas Conference. South Dakota School of Mines, Rapid City, SD.

Enhancing the Bioavailability of Subbituminous coal. Presentation by M.A. Urynowicz and Z. Huang, 2011. Goldschmidt Conference, Prague, Czech Republic.

An evaluation of various coal pretreatment agents for the stimulation of secondary biogenic coalbed natural gas. Presentation by Z. Huang. 2011. The Eight Annual Water Environment Federation and American Water Works Association Rocky Mountain Region Student Conference, University of New Mexico, Albuquerque, New Mexico.

Fermentative and Methanogenic Activity of a Coal Microbial Community. Presentation by D.M. Bagley, 2012. Biogenic Coal Bed Natural Gas Conference, Laramie, WY.

Bioconversion of Powder River Basin Subbituminous Coal: Methane Production using Permanganate as a Pretreatment Agent. Presentation by Z. Huang, 2012. Biogenic Coal Bed Natural Gas Conference, Laramie, WY.

Biogenic Methane From Coal: the oxidation factor. Presentation by L. Gallagher, 2012. Biogenic Coal Bed Natural Gas Conference, Laramie, WY.

Ethanol Conversion to Methane by a Coal Microbial Community. Presentation by D.M. Bagley, 2012. Biogenic Coal Bed Natural Gas Conference, Laramie, WY.

Sulfate reduction and methanogenesis in coal microcosms. Presentation by A.W. Glossner, L. Gallagher, L. Landkamer, L. Figueroa, J. Munakata-Marr and K.W. Mandernack, 2012. Goldschmidt Conference, Montreal, Canada.

References:

Ahmed, M. and J. W. Smith (2001). Biogenic methane generation in the degradation of eastern Australian Permian coals. *Organic Geochemistry* 32: 809-816.

Amy, G., Drewes, J. (2007). Soil aquifer treatment (SAT) as a natural and sustainable wastewater reclamation/reuse technology: Fate of wastewater effluent organic matter (EfOM) and trace organic compounds. *Environmental Monitoring and Assessment* 129: 19-26.

Aravena, R., S. M. Harrison, J. F. Barker, H. Abercrombie and D. Rudolph (2003). Origin of methane in the Elk Valley coalfield, southeastern British Columbia, Canada. *Chemical Geology* 195(1-4): 219-227.

Bhattacharya, S. K., Sluder, J. L., and Uberoi, V. (1995). Effects of 4-nitrophenol on H_2 and CO levels in anaerobic propionate systems. *Water Research* **29**, 1249-1258.

Boone, D. R. (1990). Ecology of methanogenesis, American Society of Microbiology, Washington D.C..

Budde, W. L. *Analytical Mass Spectrometry: Strategies for Environmental and Related Applications*. Oxford University Press: Oxford, NY, 2001; pp 82-85.

Catcheside, D. e. A. and J. P. Ralph (1999). Biological processing of coal. *Appl Microbiol Biotechnol* 52: 16-24.

Claypool, G. E. (2001). Geochemical Characterization of Biogenic Gas and Coalbed Methane in Shallow Gas Fields: Eastern Denver Basin, Powder River Basin and Williston Basin: 29.

Cohen, M. S. and P. D. Gabriele (1982). Degradation of Coal by the Fungi *Polyporus versicolor* and *Poria monticola*. *Applied and Environmental Microbiology 44(1): 23-27.*

Conti, J. J., P. D. Holtberg, J. A. Beamon, A. S. Kydes and G. E. Sweetnam (2006). *Annual Energy Outlook 2006*. Energy Information Administration: 236.

Depoi, F. S.; Pozebon, D.; Dikalkreuth, W. D., Chemical characterization of feed coals and combustion-by-products from Brazilian power plants. *International Journal of Coal Geology* 2008, 76, 227-236.

Dowling, N. J. E., Nichols, P. D., and White, D. C. (1988). Phospholipid fatty acid and infra-red spectroscopic analysis of a sulphate-reducing consortium. *FEMS Microbiology Letters* **53**, 325-333.

Ehrmann, B. M.; Robbins, W. K.; Rodgers, R. P.; Marshall, A. G., Asphaltene Co-Precipitate Molecular Progression as a Function of Soxhlet Extraction Period, Illuminated by Negative ESI FT-ICR MS. ASMS Salt Lake City, UT. May 2010.

Faison, B. D. (1991). Microbial Conversion of Low Rank Coals. *Nature Biotechnology* 9: 951-956.

Faiz, M. and P. Hendry (2006). Significance of microbial activity in Australian coal bed methane reservoirs -- a review. *Bulletin of Canadian Petroleum Geology* 54(3): 261-272.

Fakoussa, R. M. (1981) Coal as a substrate for microorganisms: investigations of the microbial decomposition of untreated hard coal. Bonn, Germany, University of Bonn, Ph.D.

Fakoussa, R. M. and M. Hofrichter (1999). Biotechnology and microbiology of coal degradation. *Applied Microbiology and Biotechnology* 52(1): 25-40.

Formolo, M.; Martini, A.; Petsch, S. (2008). Biodegradation of sedimentary organic matter associated with coalbed methane in the Powder River and San Juan Basins, U.S.A. *International Journal of Coal Geology*. 76: 86-97.

Harris, S. H., Smith, R. L., and Barker, C. E. (2008). Microbial and chemical factors influencing methane production in laboratory incubations of low-rank subsurface coals. *International Journal of Coal Geology* 76: 46-51.

Holker, U., S. Ludwig, T. Scheel and M. Hofer (1999). Mechanisms of coal solubilization by the deuteromycetes Trichoderma atroviride and Fusarium oxysporum. *Appl Microbiol Biotechnol* 52: 57-59.

Ivanov, I. P. (2005). Main trends in the biotechnological processing of coals: A review. *Solid Fuel Chemistry* 1: 3-10.

Jaffrennou, C., Stephan, L., Giamarchi, P., Cabon, J., Burel-Deschamps, L., Bautin, F. (2007). Direct fluorescence monitoring of coal organic matter released in seawater. *Journal of Fluorescence* 17: 564-572.

Jones, E. J. P., Voytek, M. A., Corum, M. D., and Orem, W. H. (2010). Stimulation of methane generation from nonproductive coal by addition of nutrients or a microbial consortium. *Applied and Environmental Microbiology* 76: 7013-7022.

Laborda, F., I. F. Monistrol, N. Luna and M. Fernandez (1999). Processes of liquefaction/solubilization of Spanish coals by microorganisms. *Appl Microbiol Biotechnol* 52: 49-56.

Law, B. E., D. D. Rice and R. M. Flores (1991). Coalbed gas accumulations in the Paleocene Fort Union Formation, Powder River basin, Wyoming in: Coalbed Methane of Western North America: RMAG Guidebook. RMAG Fall Conference and Field Trip, Glenwood Springs, CO.

Levine, D. G.; Schlosberg, R. H.; Silbernagel, B. G. (1982). Understanding the chemistry and physics of coal structure (A Review). *Proc. Natl. Acad. Sci.* 79: 3365-3370.

McInerney, M. J. and M. P. Bryan (1981). Anaerobic Degradation of Lactate by Syntrophic Associations of Methanosarcina barkeri and Desulfovibrio Species and Effect of H_2 on Acetate Degradation. *Applied and Environmental Microbiology* 41(2): 346-354.

McKnight, D.M., Boyer, E.W., Westerhoff, P.K., Doran, P.T., Kulbe, T., Andersen, T. (2001). Spectrofluorometric characterization of dissolved organic matter for indication of precursor organic material and aromaticity. *Limnol. Oceanogr* 46 (1), 38-48.

Miller, J. M. *Chromatography: Concepts and Contrasts*, Second Edition (2005). Wiley-Interscience: Hoboken, NJ; pp 390-411.

Nisar, J.; Awan, I. A.; Ahmad, T.; Nas, G. (2007) Analysis of aliphatic and aromatic hydrocarbons resulting from Pakistani coals by pyrolysis-gas chromatography. *J. Chem. Soc. Pakistan* 29: 247-250.

Pancost, R. D. and Sinninghe Damsté, J. S. (2003). Carbon isotopic compostitions of prokaryotic lipids as tracers of carbon cycling in diverse settings. *Chemical Geology* 195: 29-58.

Panow, A., J. M. P. FitzGerald and D. E. Mainwaring (1997). Mechanisms of biologically-mediated methane evolution from black coal. Fuel Processing Technology 52(1-3): 115.

Patidar, S. K. and Tare, V. (2005). Effect of molybdate on methanogenic and sulfidogenic activity of biomass. *Bioresource Technology* 96: 1215-1222.

Potter, M. C. (1908). Bakterien als Agentien bei der Oxidation amorpher Kohle. *Zentralblatt der Bakteriologischen Parasitenkunde II* (21): 647-665.

Rice, D. D. (1993). Composition and Origins of Coalbed Gas. *AAPG Studies in Geology* 38.

Rice, D. D. and G. E. Claypool (1981). Generation, accumulation, and resource potential of biogenic gas. *AAPG Bulletin* 65(1): 5-25.

Rittmann, B.E. and P.L. McCarty (2001). Environmental Biotechnology: Principles and Applications. McGraw-Hill Publishing Company.

Rogoff, M., H. (1962). Chemistry of Oxidation of Polycyclic Aromatic Hydrocarbons by Soil Psuedomonads. *Journal of Bacteriology* 83(5): 998-1004.

Scott, A. R. (1999). Improving Coal Gas Recovery with Microbially Enhanced Coalbed Methane. Coalbed Methane: Scientific, Environmental and Economic Evaluation. M. Mastalerz, M. Glikson and S. Golding. Dordrecht, Kluwer: 1-22.

Scott, a. R., W. R. Kaiser and W. B. Ayers (1994). Thermogenic and Secondary Biogenic Gases, San-Juan Basin, Colorado and New-Mexico - Implications for Coalbed Gas Producibility. *AAGP Bulletin* 78(8): 1186-1209.

Shumkov, S., S. Terekhova and K. Laurinavichius (1999). Effect of enclosing rocks and aeration on methanogenesis from coals. *Applied Microbiology and Biotechnology* 52(1): 99-103.

Smith, J. W. and R. J. Pallasser (1996). Microbial origin of Australian coalbed methane. *AAPG Bulletin* 80(6): 891-897.

Strapoc, D., M., C. E. Mastalerz and A. Schimmelmann (2007). Characterization of the origin of coalbed gases in southeastern Illinois Basin by compound-specific carbon and hydrogen stable isotope ratios. *Geochemistry* 38: 267-287.

Tanner, R. S., 2006. Cultivation of bacteria and fungi. In: Garland, J. L. (Ed.), *Manual of Environmental Microbiology*. ASM Press, Washington D.C.

Volkwein, J. C., A. L. Schoeneman, E. G. Clausen, J. L. Gaddy, E. R. Johnson, R. Basu, N. Ju and K. T. Klasson (1994). Biological production of methane from bituminous coal. *Fuel Processing Technology* 40(2-3): 339-345.

Whiticar, M. J., E. Faber and M. Schoell (1986). Biogenic methane formation in marine and freshwater environments: CO2 reduction vs. acetate fermentation-isotopic evidence. *Geochimica et Cosmochimica Acta* 50: 693-709.

APPENDIX 1

AMDIS results for Durango Coal extract

Soxhlet extraction

RT(min)	Chemical Name
3.2279	Octane (ID# 111-659)
3.661	Octane (ID# 111-659)
4.1132	Octane (ID# 111-65 9)
4.2563	Nonane (ID# 111-842)
4.4228	Nonane (ID# 111-842)
4.9863	Octane (ID# 111-659)
5.2052	Nonane (ID# 111-842)
5.2252	Nonane (ID# 111-842)
6.4896	Nonane (ID# 111 842)
7.2652	Nonane (ID# 111-842)
7.2686	Nonane (ID#111-842)
8.0973	Undecane (ID# 1120-21 4)
12.0867	Decane (ID#12418-5)
12.7627	Undecane (ID# 1120-21-4)
13.7545	Undecane (ID# 1120-21-4)
14.7463	Undecane (ID# 1120-21 4)
14.8699	Undecane (ID# 1120-21 4)
15.0172	Undecane (ID#112D-21 4)
15.2689	Undecane (ID# 1120-21 4)
16.3837	Undecane (ID# 1120-21 4)
16.9701	Undecane (1D# 1120-21 4)
17.3265	Dodecane (ID# 112403)
18.7105	Dodecane (ID#112403)
19.5913	Dodecane (ID#112403)
19.8988	Tndecane (ID#62950-5)
21.3386	Tridecane (ID# 629 50-5)
21.5119	Tndecane (ID#62950-5)
21.5771	Undecane (ID# 1120-21 4)
22.2692	Tridecane (ID# 629 50-5)
23.4961	Tridecane (ID# 629 50-5)
23.7996	Tridecane (ID# 629 50-5)
24.6386	Tetradecane (ID# 629-594)
26.0077	Hexadecane (ID# 544 76-3)
26.0086	Tridecane (ID# 629 50-5)
26.0199	Tridecane (ID# 629 50-5)
26.8058	Tridecane (ID# 629 50-5)
28.0965	Hexadecane (ID# 544 76-3)
28.8251	Hexadecane (ID# 544 76-3)

29.7659	Tridecane (ID# 629 50-5)
30.0388	Octadecane (ID# 8593-453)
30.7271	Heptadecane (ID# 8629187)
30.8404	Nonadecane (ID# 629925)
30.8404	Hexadecane (ID# 544 76-3)
32.5268	Octadecane (ID# 593-453)
34.2383	Nonadecane (ID# 629 925)
35.8703	Octadecane (ID# 593-453)
35.8703	Heptadecane (ID#8629187)
37.4293	Heneicosane (ID# 8629947)
38.923	Octadecane (ID# 593-45 3)
38.923	Docosane (ID# 629970)
40.3554	Heneicosane (ID# 629947)
40.3554	Tricosane (ID# 638 67-5)
41.7308	Tetracosane (1DB 646-31 1)
41.7308	Heneicosane (ID# 629947)
41.7326	Heptadecane (ID# 629187)
43.0528	Docosane (ID# 629-970)
44.3294	Hexacosane (ID# 630-01 3)
44.3303	Heneicosane (ID# 629947)
45.5572	Heptacosane (ID# 593-497)
46.7465	Octadecane (ID#593-453)
47.8976	Pentcosane (ID# 629992)
47.8976	Docosane (ID# 629-970)
50.0951	Nonadecane (ID# 629925)

AMDIS results for extraction of Big George coal

Soxhlet		Microwave	
RT (min)	Chemical Name	RT(min)	Chemical Name
16.3106	Undecane (ID# 1120-21 4)	14.9042	Undecane (ID# 1120-21 4)
19.5227	Dodecane (ID# 112403)	16.3099	Undecane (ID# 1120-21 4)
19.5313	Dodecane (ID#112403)	19.5244	Dodecane (ID# 112403)
22.2094	Tridecane (ID# 629 50-5)		Tridecane (ID# 629 50-5
	Undecane (ID# 1120-21 4)	19.5298	Dodecane (ID# 112403)
	Dodecane (ID# 112403)		Undecane (ID# 1120-21 4)
22.2136	Tridecane(ID# 62950-5)	22.2085	Tridecane (ID# 629 50-5)
	Undecane (ID# 1120-21-4)		Undecane (ID# 1120-21 4)
30.799	Heptadecane (ID# 629187)		Dodecane (ID# 112403)
	Tridecane (ID# 629-50-5)	22.2113	Tridecane (ID# 62950-5)
	Hexadecane (ID# 544-76-3)		Undecane(ID# 1120-21-4)
34.1897	Nonadecane(ID# 629925)		Dodecane (ID# 112403)
	Hexadecane(ID#544 76-3)	30.799	Tridecane (ID# 629 50-5)
	Heptadecane (ID# 629187)		Octadecane (ID# 593-453)
	Octadecane (ID# 593-453)	34.185	Nonadecane (ID# 629-92-5)
	Tridecane (ID# 629 50-5)		Heptadecane (ID# 629187)
37.3844	Heptadecane (ID# 629787)		Octadecane (ID# 593-453)
	Heneicosane (ID# 629947)		Hexadecane (ID# 544 76 3)
	Octadecane (ID# 593-453)		Heneicosane (ID# 629947)
	Nonadecane (ID# 629-92-5)	34.1859	Heptadecane (ID# 629187)
37.3844	Heneicosane (ID# 629947)		Hexadecane(ID# 544 76-3)
	Heptadecane (ID# 629187)		Octadecane (ID# 593-453)
	Octadecane (ID# 593-453)		Nonadecane (ID# 629925)
	Nonadecane (ID# 629 925)		Tridecane (ID# 629 50-5)
	Hexadecane (ID# 544 76-3)		Pentadecane (ID# 629-6)9)
38.8762	Pentadecane (ID# 629-629)		Heneicosane (ID# 629947)
	Heptadecane (ID# 629187)	37.3796	Heneicosane (ID# 629947)
	Octadecane (ID# 593-453)		Nonadecane (ID# 629 925)
40.3037	Tricosane (ID# 63867-5)		Octadecane (ID# 593-453)
	Octadecane (ID# 593-453)		Heptadecane (ID# 629187)
	Honoicosane (ID# 629947)	40.3057	Tricosane (ID# 63867-5)
	Nonadecane (ID# 629 925)		Nonadecane (ID# 629 925)
	Heptadecane (ID# 629787)		Heneicosane (ID# 629947)
	Hexadecane (ID# 544 76-3)		Octadecane (ID# 593-453)
	Ficosane (ID# 112-95-8)		Heptadecane (ID# 629187)
	Docosane (ID# 629-97-0)		Hexadecane (ID# 54476-3)
41.6839	Hepadecane (ID# 62978 7)	40.3057	Heneicosane (ID# 629947)
	Octadecane (ID# 593-45-3)		Nonadecane (ID# 629 925)

43.0075	Docosane (ID# 629-97-0)
	Honoicosane (ID# 629 947)
	Heptadecane (ID# 629 787)
	Octadecane (ID# 593-453)
	Nonadecane (ID# 629925)
	Pentacosane (ID# 629 992)
	Hexadecane (ID# 544 76 3)
	Tetracosane (ID# 646-31 1)
44.2832	Ocadecane(ID# 593-453)
	Hoptadecane (D# 629187)
	Nonadocane (ID# 629925)
	Heneicosane (ID#629 947)
	Hexadecane(ID# 544 76-3)
	Docosane (ID# 629-97-0)
	Hexacosane (ID# 630-01 3)
	Tricosane (ID# 638 67-5
	Pentcosane (ID11 6)9 992)
45.5153	Docosane (ID#629970)
	Heptacosane (ID# 593-497)
	Tricosane (ID# 638 67-5
	Heneicosane (ID# 629 947)
	Nonadecane (ID# 629 925)
	Octadecane (ID# 593-453)
	Heptadecane (ID# 629787)
	Tetracosane (ID# 64631 1)
	Hexadecane (ID# 544 76-3)
45.5153	Heptacosane (ID# 593-497)
	Docosane (ID# 629 97 0)
	Tricosane (ID# 638 67-5
	Nonadecane (ID# 629925)
	Honoicosane (ID#629 947)
	Octadecane (ID# 593-453)
	Heptadecane (ID# 629187)
	Tetracosane (ID# 64631 1)
46.7024	Heptadecane (ID# 629187)
	Octadecane (ID# 593-453)
46.7035	Octadecane (ID# 593-453)
	Heptadecane (ID# 629787)
	Nonadecane (ID# 629925)
47.8546	Docosane (ID# 629-970)
	Pentacosane (ID# 629-99-2)
	Hexacosane (ID# 630-01 3)
	Heneicosane (ID# 629947)
	Tricosane (ID# 638 67-5)
	Octadecane (ID# 593-453)
	Heptadecane (ID# 629187)
40.3057	Tricosane (ID# 638 67-5)
	Heneicosane (ID# 629947)
	Octadecane (ID# 593-453)
	Nonadecane (ID# 629925)
	Heptadecane (ID# 629787)
	Docosane (ID# 629-970)
41.6819	Octadecane (DO 593-453)
	Heptadecane (DO 629187)
	Hexadecane (ID# 544-76-3)
	Docosane (ID# 629-97-0)
43.0066	Pentscosane (ID# 629992)
	Docosane (ID# 629-970)
	Tricosane (ID# 638 67-5
	Heneicosane (ID# 629947)
	Tetracosane (ID# 64631 1)
	Heptadecane (ID# 629787)
	Octadecane (ID# 593-453)
	Nonadecane (ID# 629925)
44.2792	Hexacosane (ID# 630-01 3)
	Octadecane (ID# 593-453)
	Nonadecane (ID# 629 925)
	Heneicosane (ID# 629947)
	Docosane (ID# 629-970)
	Heptadecane (ID# 629187)
	Tricosane (ID# 638 67-5
	Hexadecane (ID# 544 76-3)
	Pentcosane (ID# 629992)
45.5145	Heptacosane (ID# 593-497)
	Docosane (ID# 629 97 0)
	Tricosane (ID# 63867-5)
	Heneicosane (ID# 629947)
	Pentacosane (ID# 629992)
	Hexacosane (ID# 630-01-3)
	Heptadecane (ID# 629187)
	Nonadecane (ID# 629925)
	Tetracosane(ID# 64631 1)
	Octadecane (ID# 593-453)
46.7031	Octadecane (ID# 593-453)
	Heptadecane (ID# 629187)
	Nonadecane (ID# 629925)

	Heptacosane (ID# 593-497)	46.7031	Octacosane (ID# 630-02-4)
	Octadecane (ID# 593-453)	47.8537	Docosane(ID# 629970)
	Nonacosane (ID# 630-03-5)		Pentacosane (ID#629992)
51.16	Heptadecane (ID# 629187)		Tricosane (ID# 638 67-5)
	Octadecane (ID# 593-453)		Heptacosane (ID# 593-497)
			Heneicosane (ID# 629947)
			Nonacosane (ID# 630-035)
		48.9748	Octadecane (ID# 593-45 3)
			Heptadecane (ID# 629787)

AMDIS results for extraction of Big George coal

Oven		Soxhlet	
RT(min)	Chemical Name	RT (min)	Chemical Name
16.3112	Undecane (ID#112-21 4)	16.3106	Undecane (ID# 1120-21 4)
16.3147	Undecane (ID# 1120-21 4)	19.5227	Dodecane (ID# 112403)
19.525	Dodecane (ID# 112403)	19.5313	Dodecane (ID#112403)
	Undecane (ID# 1120-21 4)	22.2094	Tridecane (ID# 629 50-5)
19.5301	Dodecane (ID# 112403)		Undecane (ID# 1120-21 4)
	Undecane (ID# 1120-21-4)		Dodecane (ID# 112403)
22.21	Tridecane (ID# 629 50-5)	22.2136	Tridecane(ID# 62950-5)
	Undecane (ID# 1120-21 4)		Undecane (ID# 1120-21-4)
	Dodecane (ID# 112403)	30.799	Heptadecane (ID# 629187)
22.2143	Tridecane (ID# 629 50-5)		Tridecane (ID# 629-50-5)
	Undecane (ID# 1120-21-4)		Hexadecane (ID# 544-76-3)
29.7303	Tridecane (ID# 629 50-5)	34.1897	Nonadecane(ID# 629925)
30.7967	Octadecane (ID# 593-453)		Hexadecane(ID#544 76-3)
	Nonadecane (ID# 629 925)		Heptadecane (ID# 629187)
30.7976	Tridecane (ID# 629 50-5)		Octadecane (ID# 593-453)
	Octadecane (ID# 593-453)		Tridecane (ID# 629 50-5)
32.4779	Octadecane (ID# 593-453)	37.3844	Heptadecane (ID# 629787)
34.1909	Heptadecane (ID# 629-78-7)		Heneicosane (ID# 629947)
	Hexadecane (ID# 544-76-3)		Octadecane (ID# 593-453)
	Octadecane (ID# 593-453)		Nonadecane (ID# 629-92-5)
	Tridecane (ID# 629 50-5)	37.3844	Heneicosane (ID# 629947)
	Nonadecane (ID# 629925)		Heptadecane (ID# 629187)
	Pentadecane (ID# *629-629)*		Octadecane (ID# 593-453)
34.1909	Nonadecane(ID# 629925)		Nonadecane (ID# 629 925)
	Heptadecane (ID# 629187)		Hexadecane (ID# 544 76-3)
	Octadecane (ID# 593-453)	38.8762	Pentadecane (ID# 629-629)
	Hexadecane (ID# 544 76-3)		Heptadecane (ID# 629187)
	Tridecane (ID# 629 50-5)		Octadecane (ID# 593-453)
37.3813	Heneicosane (ID# 629947)	40.3037	Tricosane (ID# 63867-5)
	Heptadecane (ID# 629187)		Octadecane (ID# 593-453)
	Octadecane (ID# 593-453)		Honoicosane (ID# 629947)
	Nonadecane (ID# 629925)		Nonadecane (ID# 629 925)
	Hexadecane (ID# 544 76-3)		Heptadecane (ID# 629787)
40.3075	Tricosane(ID#63867-5)		Hexadecane (ID# 544 76-3)
	Octadecane (ID# 593-453)		Ficosane (ID# 112-95-8)
	Nonadecane (ID# 629 925)		Docosane (ID# 629-97-0)
	Heneicosane (ID# 629947)	41.6839	Hepadecane (ID# 62978 7)

	Docosane (ID# 629 97 0)
	Hexadecane (ID# 544 76-3)
	Heptadecane (ID# 629187)
	Eicosane (ID# 112-95-8)
41.6826	Octadecane (ID# 593-453)
43.0078	Pentacosane (ID# 629 992)
	Docosane (ID# 629 97 0)
	Tricosane (ID# 638 67-5)
	Heneicosane (ID# 629947)
	Octadecane (ID# 593-453)
	Nonadecane (ID# 629925)
	Heptadecane (ID# 629187)
	Hexadecane (ID# 544-76-3)
44.2817	Hexacosane (ID# 630-01 3)
	Octadecane (ID# 593-453)
	Nonadecane (ID# 629925)
	Docosane (ID# 629-970)
	Heneicosane (ID#629 947)
	Heptadecane (ID# 629787)
	Tricosane (ID# 638 67-5)
	Pentacosane (ID# 629 992)
	Hexadecane !ID# 544 76-3)
	Tetracosane (ID# 646-31 1)
44.2828	Octadecane (ID# 593-453)
	Hexacosane (ID# 630-01 3)
	Nonadocane (ID# 629 925)
	Heptadecane (ID# 629187)
	Henoicosane (ID# 629 947)
	Docosane (ID# 629 97 0)
	Tricosane (ID# 638 67-5
	Hexadecane (ID# 54476-3)
	Pentacosane (ID# 629 992)
45.5139	Heptacosane (ID# 593-497)
	Docosane (ID# 629-970)
	Pentcosane (ID# 629 992)
	Tricosane (ID# 638-67-5)
	Hexacosane (ID# 630-01 3)
	Henoicosane (ID# 629947)
	Nonadocane (ID# 629925)
	Octadecane (ID# 593-453)
	Hoptadecane (ID# 629787)
46.7064	Octadecane (ID# 593-453)
	Heptadecane (ID# 629187)
	Octadecane (ID# 593-45-3)
43.0075	Docosane (ID# 629-97-0)
	Honoicosane (ID# 629 947)
	Heptadecane (ID# 629 787)
	Octadecane (ID# 593-453)
	Nonadecane (ID# 629925)
	Pentacosane (ID# 629 992)
	Hexadecane (ID# 544 76 3)
	Tetracosane (ID# 646-31 1)
44.2832	Ocadecane(ID# 593-453)
	Hoptadecane (D# 629187)
	Nonadocane (ID# 629925)
	Heneicosane (ID#629 947)
	Hexadecane(ID# 544 76-3)
	Docosane (ID# 629-97-0)
	Hexacosane (ID# 630-01 3)
	Tricosane (ID# 638 67-5
	Pentcosane (ID11 6)9 992)
45.5153	Docosane (ID#629970)
	Heptacosane (ID# 593-497)
	Tricosane (ID# 638 67-5
	Heneicosane (ID# 629 947)
	Nonadecane (ID# 629 925)
	Octadecane (ID# 593-453)
	Heptadecane (ID# 629787)
	Tetracosane (ID# 64631 1)
	Hexadecane (ID# 544 76-3)
45.5153	Heptacosane (ID# 593-497)
	Docosane (ID# 629 97 0)
	Tricosane (ID# 638 67-5
	Nonadecane (ID# 629925)
	Honoicosane (ID#629 947)
	Octadecane (ID# 593-453)
	Heptadecane (ID# 629187)
	Tetracosane (ID# 64631 1)
46.7024	Heptadecane (ID# 629187)
	Octadecane (ID# 593-453)
46.7035	Octadecane (ID# 593-453)
	Heptadecane (ID# 629787)
	Nonadecane (ID# 629925)
47.8546	Docosane (ID# 629-970)
	Pentacosane (ID# 629-99-2)
	Hexacosane (ID# 630-01 3)

	Nonadecane (ID# 629925)		Heneicosane (ID# 629947)
47.8543	Docosane (ID# 629-970)		Heptacosane (ID# 593-497)
	Heptacosane (ID# 593-49-7)		Octadecane (ID# 593-453)
	Tricosane (ID# 638 67-5)		Nonacosane (ID# 630-03-5)
	Pentcosane (ID# 629 992)	51.16	Heptadecane (ID# 629187)
	Heneicosane (ID# 6)9947)		Octadecane (ID# 593-453)
	Hexacosane (ID# 630-01 3)		
	Octadecane (ID# 593-453)		
	Nonacosane (ID# 630-035)		
	Tetracosane (ID# 646-31 1)		
48.9759	Octadecane (ID# 593-453)		
	Heptadecane (ID# 629187)		
	Nonadecane (ID# 629 925)		
	Hexadecane(ID# 544 76-3)		
	Docosane (ID# 629 97 0)		